Fractal Analysis of Cardiac Dynamics: The Application of Detrended Fluctuation Analysis on Short-term Heart Rate Variability

Pandelis Perakakis

Personality, Evaluation and Psychological Treatment

Granada University

A thesis submitted for the degree of

PhilosophiæDoctor (PhD)

2009 October

Editor: Editorial de la Universidad de Granada
Autor: Pandelis Perakakis
D.L.: Gr. 156-2010
ISBN: 978-84-692-8392-9

SUPERVISOR REPORT

Dr. Jaime Vila Castellar, professor of psychology at the department of personality, evaluation and psychological treatment in the university of Granada,

Dr. Gustavo Reyes del Paso, professor of psychology at the department of personality, evaluation and psychological treatment in the university of Jaen,

Dr. Lourdes Anllo–Vento, professor of psychology at the department of personality, evaluation and psychological treatment in the university of Granada,

CERTIFY: that this doctoral dissertation entitled **Fractal Analysis of Cardiac Dynamics: The Application of Detrended Fluctuation Analysis on Short-term Heart Rate Variability**, was written by Pandelis Perakakis under our supervision and fulfills the qualitative criteria required for its defense.

1st of October 2009

Jaime Vila Castellar
Gustavo Reyes del Paso
Lourdes Anllo–Vento

Στην Αγαπημένη μου Γιαγιά

Acknowledgements

The ideas and results presented in this doctoral dissertation represent the Ithaca of an exciting four-year academic and personal adventure. Unfortunately, there is no space here to describe the marvelous journey that lead to this thesis. Perhaps, the only thing I can do is to remember a few of the people that have accompanied and shared with me all the wonderful and difficult moments.

First of all, I would like to acknowledge the guidance and support of my supervisors Jaime Vila, Gustavo Reyes and Lourdes Anllo-Vento. Especially Jaime has been a continuous motivation to stay on the academic track, providing an outstanding example both as a scientist and as a person. He is the academic father of a wonderful family, the group of human psychophysiology in the University of Granada, of which I have been a member for the last seven years. This thesis was only possible thanks to all of them.

The most interesting aspect of my academic life these past years has been without doubt the opportunity it gave me to travel and meet exciting cultures and remarkable people. In Madrid, I met my good friend and scientist Michael Taylor with whom I started discussing about nature's complexity during our unforgettable gastronomical orgies at my regular weekend visits. In Rio de Janeiro, "La Ciudad Maravillosa", I had the opportunity to meet and collaborate with professors Eliane Volchan, Walter Machado Pinheiro and all the wonderful and talented people in their research groups. In Moscow, I was kindly welcomed to the Buetyko clinic by Dr. Andrey Novozhilov. Finally, in Boston I was warmly received by professor Eugene Stanley in the Center of Polymer Studies at Boston University, where I had the pleasure to enjoy interesting conversations with professor Plamen Ivanov.

On a more personal note I wish to thank Chara Theologidou for being always next to me in so many different ways throughout the years and Michael Vousdouka for the “finals” and the innumerable discussions about “Life, the Universe and Everything”. Along with them comes a long list of beautiful people around the world with whom I laughed, cried, made love, played music, travelled and talked for hours with a mind blurred from wine or stimulated by a hot cup of coffee. They know who they are and I thank them for the magic.

Last, I wish to dedicate this effort to my family, at my hometown Thessaloniki in Greece. Although I have spent all these years away from them, I always recognize their presence in anything I do or feel. They are who I am and I owe them everything.

Abstract

Fractal measures of heart rate variability have been proposed as complementary to time and frequency domain indices and, in many cases, have proven to be valid predictors of cardiovascular disease. However, their relationship with respiratory parameters and more common health indicators such as vagal tone is still not clear. In this doctoral dissertation, we examine the effect of breathing frequency, average heart period and pharmacological parasympathetic blockade on the fractal properties of short-term cardiac dynamics. Heart period analysis is performed with a mathematical software (KARDIA) developed for the purpose of our studies, which is also presented in this thesis. The results of our first study revealed that: 1) the periodical properties of RSA produce a change of the correlation exponent in HRV at a scale corresponding to the respiratory period, 2) the short-term DFA exponent is significantly reduced when breathing frequency rises from 0.1Hz to 0.2Hz. In the second study atropine was administered to six healthy males in a controlled laboratory setting. Parasympathetic blockade produced a significant increase in the α_1 scaling exponent assessed by detrended fluctuation analysis. We showed that this was produced by smooth local trends in the data, rather than an alteration in underlining dynamics. Our results call attention to a methodological and conceptual problem related to the application of fractal measures to a limited range of scales in which single physiological control mechanisms exert a dominant influence.

Contents

List of Figures

LIST OF FIGURES

List of Tables

Glossary

α scaling exponent obtained by DFA

α_1 short-term scaling exponent usually calculated for the range between 4 and 16 heartbeats

α_2 long-term scaling exponent usually calculated for the range between 17 and 64 (or more) heartbeats

1/f noise also pink noise; a signal or process with a frequency spectrum such that the power spectral density is inversely proportional to the frequency

ANS Autonomous nervous system

DFA Detrended Fluctuation Analysis; algorithm used to quantify long-term correlations in nonstationary time series

DFT Discrete Fourier transform

ECG Electrocardiogram

ERP Event-related Potentials

Fractal a rough or fragmented geometric shape that can be split into parts, each of which is (at least approximately) a reduced-size copy of the whole

HF High frequency spectral power

hr hours

HRV Heart rate variability; the variation in the period between heartbeats that is measured as an index of autonomic control on the heart

IBI Interbeat interval

LF Low frequency spectral power

min minutes

ms milliseconds

N Normal heartbeat as opposed to ectopic beats or other artifacts

NN Time interval between normal heartbeats

NN50 Absolute count of differences between successive NN intervals greater than 50 ms

PCR Phasic cardiac responses

pNN50 Proportion of differences between successive NN intervals greater than 50 ms

RMS Root mean square

RMSSD Root mean square of successive differences

RSA Respiratory sinus arrhythmia; a naturally occurring variation in heart rate that occurs during a breathing cycle

Scale invariance also Self-similarity; property of objects (geometrical shapes or fluctuating time series) that do not change if length scales (or energy scales) are multiplied by a common factor

Scaling crossover Change in scaling properties of HRV correlations usually due to persistent trends in the data

SDANN Standard deviation of sequential 5 min heartbeat interval means

SDNN Standard deviation of heartbeat intervals

SOC Self-organized criticality; theory proposed to explain why certain physical and biological systems exhibit long-range power-law correlations

ULF Ultra low frequency spectral power

VLF Very low frequency spectral power

Chapter 1

Introduction

The variability in the heart rate signal (Heart Rate Variability; HRV) is extensively being studied as an indirect index of autonomic regulation. In psychophysiological experiments, measures of HRV in resting states are used to elucidate the relationship between autonomic state and cognitive performance or emotional responses. Moreover, HRV indices have repeatedly proven useful in distinguishing cardiovascular patients from healthy populations. Despite their ample use in diverse fields, there are clear methodological problems associated with the estimation and interpretation of HRV measures. Available HRV metrics are continuously being refined and new techniques introduced. In recent years, the study of HRV has attracted the interest of statistical physicists who observed a resemblance of HRV fluctuations to complex signals deriving from physical systems characterized by nonlinear dynamics.

This discovery of nonlinearities in HRV triggered a series of studies with remarkable results. Various investigations confirmed that long-term HRV fluctuations are not random, but exhibit long-term correlations that do not exhibit any characteristic scale, but are rather "scale invariant". This type of scale invariant variability is also known as fractal and the methodology employed to evaluate it is often called fractal analysis. It was discovered that the fractal organization of HRV fluctuations is distorted in cardiovascular patients and elderly populations. One of the most popular algorithms applied to HRV signals in order to reveal these complex fractal fluctuation patterns is the Detrended Fluctuation Analysis (DFA). DFA was introduced in 1995 and has been used since then in more than 700 HRV studies.

1. INTRODUCTION

One of the interesting findings resulting from the application of DFA to human HRV, was the clear distinction between the characteristics of long and short-term HRV fluctuation patterns. While long-term HRV shows similarities to critical physical systems, short-term HRV fluctuations are characterized by strong correlations that indicate a different organization of the underlining control mechanisms. It was hypothesized that strong correlation patterns in short-term HRV are due to the smooth heart rate oscillations associated with breathing, a phenomenon known as Respiratory Sinus Arrhythmia (RSA). Nevertheless, no experimental study properly addressed this hypothesis. On the contrary, all published investigations reporting results on short-term DFA, attribute their findings in the underlining organization of cardiac dynamics, without considering RSA in their interpretations. Therefore, despite the important number of publications examining short-term DFA exponents, the physiologic significance of this index remains elusive.

In this dissertation we experimentally tested the hypothesis that short-term DFA exponents are sensitive to RSA and therefore to breathing parameters. The findings in our first study, confirmed this hypothesis and clarified the physiological significance of this new HRV measure. In a second experiment, we tested our interpretation by comparing subjects with impaired autonomic control induced by drug administration, and control individuals. The results re-confirmed our hypotheses and further supported the mathematical and physiological interpretation of the effects of RSA and generally smooth systematic trends on the application of fractal measures to short-term HRV.

The conclusions drawn from our studies question the interpretation of results obtained by the application of DFA to short-term HRV, based on underlining fractal properties. On the contrary, we assert that DFA can be used to assess the fractal properties of long-term HRV. We discuss the potential benefits of this line of research for our theoretical understanding of physiologic control and for the clinical diagnosis of cardiovascular disorders. In terms of theoretical understanding, fractal physiology questions the paradigm of homeostasis that has been central to physiology in the last century and which postulates that physiological systems normally operate to reduce variability and maintain a constancy of internal function. Instead, fractal physiology suggests that internal feedback mechanisms produce a complex variability that renders the system more flexible and adaptive to external perturbations. In terms of clinical diagnosis, small deviations from fractal organization in cardiac dynamics could prove a

sensitive index of impaired autonomic regulation, long before the actual cardiovascular disorder manifests with clear symptoms.

We begin this thesis with a theoretical introduction of related concepts. In the second chapter we introduce the concept of HRV and review some of the most common measures. The third chapter presents the concept of fractal analysis applied to temporal processes. What follows are three articles that were submitted to highly-esteemed academic journals. The fourth chapter presents KARDIA, a software program developed for the analysis of cardiac data used in this dissertation. This paper was accepted for publication by the journal Computer Methods and Programs in Biomedicine. The fifth chapter introduces the details of the Detrended Fluctuation Analysis algorithm and describes our first study exposing the breathing frequency bias in the fractal analysis of short-term HRV. This article was published in Biological Psychology (vol.82, pp.82–88). The sixth chapter is a presentation of our second study on the effects of parasympathetic blockade on DFA, which further supports the findings and interpretation of the first study. This paper was submitted to the Journal of Cardiovascular Electrophysiology. We conclude with a discussion of our results and their implications for future research.

Chapter 2

Heart Rate Variability

In healthy individuals heart rate is neither constant nor periodic. Instead, the variability in heart rate fluctuations is determined by the complex dynamics of the sympathetic and the parasympathetic branches of the autonomic nervous system (ANS), which interact at the impulse generating tissue located in the right atrium of the heart (sinoatrial node). Generally, sympathetic stimulation increases heart rate, while parasympathetic stimulation decreases it. Heart rate variability is a composite of numerous influences reflecting physiological regulatory mechanisms. In the recent past there has been a spurt of research efforts involving HRV, based on the conviction that disentangling the sources of variation in cardiac dynamics will provide valuable information on the cardiovascular autonomic regulation of the heart.

2.1 Time Domain Measures

In time domain analysis of HRV the intervals between successive normal R waves in the electrocardiogram are measured over the period of recording (3). A variety of statistical metrics can be calculated from the intervals directly and others can be derived from the differences between intervals. The square root of variance (SDNN) is probably the most popular time domain measurement of HRV. A significant part of the variance of this measurement (30-40%) is attributed to day-night differences in the NN intervals (N stands for normal heartbeat as opposed to ectopic beats or other artifacts). Therefore, long ECG recordings (at least 18-hr) are required for its correct estimation (3). The standard deviation of the 5-min average NN intervals (SDANN) is another version of

the same measurement, although it is much smoother and less sensitive to unedited artifacts, missed beats and ectopic complexity (4). Both of these parameters are more sensible to slow trends in the heart rate data and are therefore used to quantify long-term fluctuations.

The square root of the mean squared differences of successive NN intervals (RMSSD), the absolute count of differences between successive NN intervals greater than 50 ms (NN50), and the proportion of differences greater than 50 ms (pNN50), are the most common variables calculated as differences between normal R-R intervals. In general, time domain measures derived from the differences between successive heartbeats have shown to correlate well with vagal activity and are mostly used to quantify parasympathetic modulation of cardiac dynamics (5). RMSSD is a metric that is sensitive to fast frequency heart rate fluctuations (6). It correlates significantly with frequency domain measures of HRV that quantify the power of rapid oscillations in the heart rate signal. Pharmacological blockade studies further indicate that the RMSSD statistic is sensitive to vagal cardiac control, and it has even been suggested to be superior to spectral methods as it may be less sensitive to variations in respiratory patterns (7). This notion, however, has been criticized in a recent study which revealed that the RMSSD statistic is biased by basal heart period and that between-subjects correlations of absolute levels of RMSSD and high frequency spectral variability were higher than within-subjects changes in these measures (6).

2.2 Frequency Domain Measures

Time domain indices of HRV provide statistical information on total variability over a period of time, without resolving it further. Frequency domain indices on the other hand provide information on the distribution of HRV power as a function of frequency. Power spectral analysis of short segments (usually around 5 min) of beat-to-beat HRV, either based on fast Fourier transformation or on autoregression techniques, is probably the most common frequency domain measure. This type of short-segment analysis usually reveals three peaks in distinct bands in the power spectra. The high frequency (HF) band (0.15 to 0.4 Hz) reflects respiratory modulation via efferent impulses on the cardiac vagus nerves and is abolished by parasympathetic blockade (8). It has been shown that when breathing frequency changes, the center frequency of the HF

peak is displaced according to the respiratory rate. In addition, HF variability is also completely abolished during breath holding tasks (9). The low frequency (LF) spectral band (0.04 to 0.15 Hz) is modulated by baroreflexes with a combination of sympathetic and parasympathetic efferent nerve traffic to the sinoatrial node (10; 11; 12; 13; 14; 15). Standing or head up tilt causes a modest increase in LF power and a substantial decrease in HF power (14). Atropine almost abolishes the LF peak, and beta blockade prevents the increase caused by standing up. Various manipulations of HF and LF power or the use of LF/HF ratio have been pursued in an attempt to estimate sympathetic activity. These manipulations are based in a simplistic understanding of autonomic interactions and in most cases have not led to satisfying results (3). Finally, the mechanism responsible for the very low frequency (VLF) spectral band (0 to 0.04 Hz) is a matter of dispute. VLF power is also abolished by atropine, suggesting that it uses a parasympathetic efferent limp (15). It has also been suggested that the VLF power reflects the activity partly of the renin-aldosterone system and partly thermoregulation or vasomotor activity (16).

The spectral analysis of 24-hr heart rate recordings reveals information about much slower oscillations than those observed in a 5-min recording. The lowest frequency band in the 24-hr power spectrum is the ultra low frequency (ULF) band (0 to 0.003 Hz), which quantifies fluctuations in R-R intervals with periods between 5 min and 24 hrs. The physiological basis for these slow oscillations in the heart rate is less clear. ULF indices, however, have proven to be powerful risk predictors in cardiovascular diseases (17).

2.3 Nonlinear Measures

Time and frequency domain measures of HRV quantify the variability of heart rate fluctuation in characteristic time scales. Nonlinear measures on the contrary attempt to quantify the structure or complexity of the R-R interval time series. A common linear measure, for example, would not be able to distinguish between a random, a periodic and a normal series of R-R intervals if all three had the same standard deviation. These three types of signals, however, have a totally different underlying organization, which may be more informative about autonomic regulation than the variation in an individual frequency band (3).

2. HEART RATE VARIABILITY

The interest in the nonlinear analysis of HRV was motivated by the demonstration of nonlinearities in the R-R interval time series, resulting by the complex interactions and the numerous feedback loops that ultimately determine the sympathetic and vagal cardiac outflow. According to many researchers, the extraordinary complexity, nonlinearity and nonstationarity generated by living organisms and present in the cardiac dynamics, as well as in many other physiological systems, defy traditional mechanistic approaches based on homeostasis and conventional bio-statistical methodologies (2; 18; 19; 20; 21; 22). It is already a widespread belief that physiological time series contain more information than can be assessed by common statistical indices and that applying concepts from statistical physics and complexity science to a wide range of biomedical problems, from molecular to organismic levels, may provide us with important insights on how physiological complex systems work (2).

A large number of nonlinear indices of HRV has been studied and new are developed continuously. Only a few of them, however, have shown a clear clinical utility. One of them is the power law slope which is obtained by the spectral power measured over 24 hrs. The spectral power will show a progressive exponential increase in amplitude with decreasing frequency. This is the characteristic $1/f$ or "pink" noise observed in complex biological systems which do not exhibit any characteristic scale (scale invariant or fractal) (1; 23). This relationship can be also plotted as the log of power versus the log of frequency, which transforms the exponential curve to a line whose slope can be estimated. In a log-log plot, the power law function between 10^{-2} Hz and 10^{-4} Hz is linear with a negative slope, and reflects the degree to which the structure of the R-R interval time series is self similar over a scale of minutes to hours (3). Decreased power law slope is a marker for increased risk of mortality after myocardial infarction (24).

Nonlinear measures of heart rate variability also include the analysis of the Poincarè plots, Lyapunov exponent, fractal dimension, approximate entropy, heart rate turbulence and many others, but these indices have not been that broadly investigated or correlated with other health measures (25).

Both linear and nonlinear measures of HRV have been used to quantify risk in a wide variety of both cardiac and noncardiac disorders such as stroke, multiple sclerosis, end stage renal disease, neonatal distress, diabetes mellitus, ischemic heart disease, myocardial infarction, cardiomyopathy patients awaiting cardiac transplantation, valvular heart disease, and congestive heart failure. HRV analysis has also been used to assess

the autonomic effects of drugs, including beta blockers, calcium blockers, psychotropic agents, antiarrhythmics and cardiac glycosides (3).

Chapter 3

Fractal Variability

Contrary to the common notion that physiological systems, including the healthy heartbeat, are regulated according to the classical principal of homeostasis, operating to reduce variability and to achieve an equilibrium-like state, it has been shown that, under normal conditions, beat-to-beat heart rate fluctuations display the kind of fractal-like, long-range correlations typically exhibited by complex nonlinear systems. On the other hand, heart rate time signals of patients with severe congestive heart failure show a breakdown of this long-range correlation behavior (26). In the next paragraphs we introduce the concept of fractal variability as it is being applied both in spatial structures and temporal processes.

3.1 Fractals in Space and Time

3.1.1 Geometrical Fractals

When applied to geometrical shapes, the term "fractal" describes objects consisting of parts that are (at least approximately) reduced copies of the whole. This means that same or similar patterns are observed under different magnifications of the original object. In other words, a fractal object is "self-similar" because looking closely at smaller regions reveals a scaled version of the whole object (23). Figure 3.1 shows a famous mathematical fractal known as the Mandelbrot set, which results from the iteration of the quadratic polynomial $z_{n+1} = z_n^2 + c$. It can be clearly observed that zooming in any of the smaller structures composing the set will reveal patterns similar to the entire object.

One could argue that fractals are mathematical, abstract structures that have nothing to do with reality. Nothing, however, could be further from truth. Nature is full with shapes exhibiting self-similarity. Common examples are lighting discharges, trees, coastlines, snow flakes, crystals, lungs (27), cell membranes (28), the Purkinje fibers in the heart, pulmonary and blood vessels and more (1).

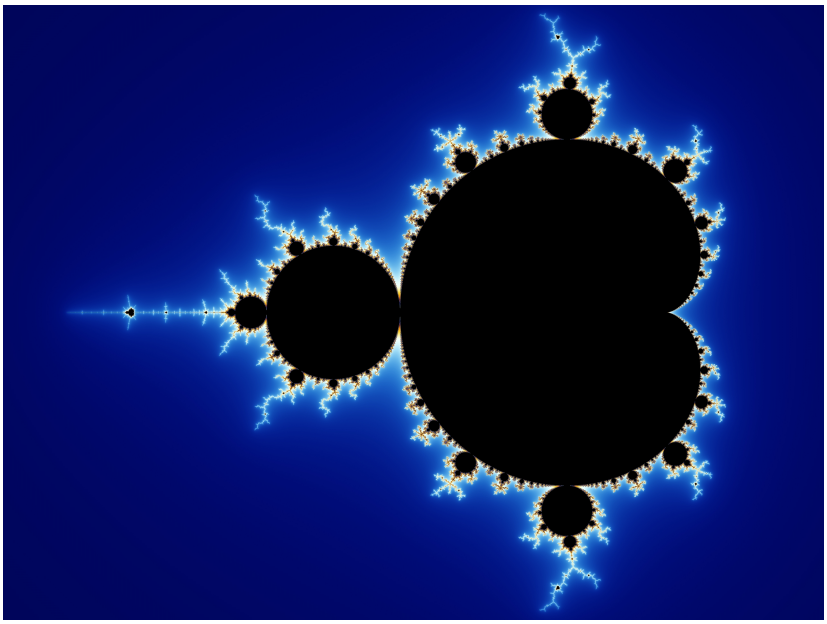

Figure 3.1: The Mandelbrot set. A mathematical fractal defined as a set of points in the complex plane resulting by the iteration of the quadratic polynomial $z_{n+1} = z_n^2 + c$

.

3.1.2 Temporal Fractals

The concept of self-similarity can be extended to fluctuating time series. Figure 3.2 shows how a temporal process, such as the healthy heart rate, can exhibit similar statistical behavior at different time scales. In this case, similarity is not structural or geometrical, but statistical. Signals demonstrating this type of temporal fractal variability have been repeatedly observed and studied in physical systems near phase transition. There is accumulating evidence, however, that biological systems also produce fractal time series, known as "scale invariant", because they "look" the same at different temporal scales. Typical examples are the healthy heart rate, the activity of

neural networks, the evolution and extinction of ecosystems and more (1).

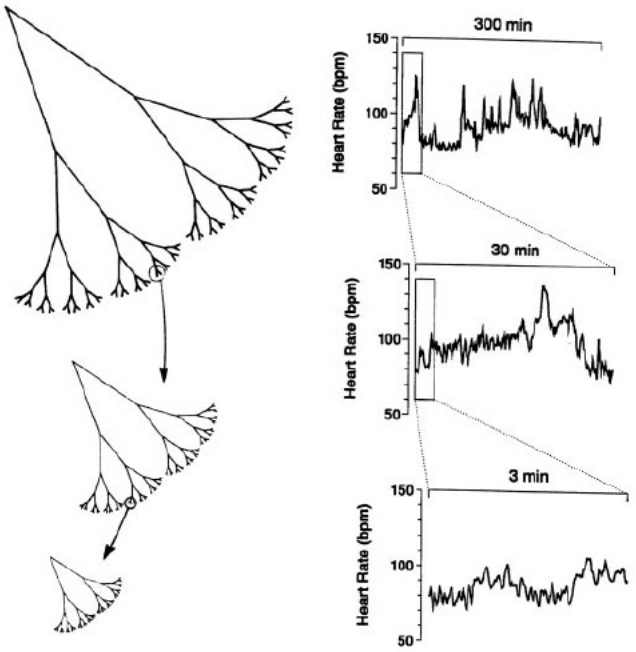

Figure 3.2: Schematic representations of self-similar structures and self-similar fluctuations. The tree-like, spatial fractal (Left) has self-similar branchings, such that the small-scale structure resembles the large-scale form. A fractal temporal process, such as healthy heart rate regulation (Right), may generate fluctuations at different time scales that are statistically self-similar

Scale invariance is a characteristic property of power law distributions. Let us consider the following function:

$$P(f) = Cf^{\alpha} \tag{3.1}$$

Let us assume that this function represents the power spectrum of a signal as a function of its frequency, where P is the power, C and α are real and constant (α being smaller than zero) and f is a variable representing the frequency. This distribution is called power law distribution because of the exponent α. In this type of functions, scale invariance becomes evident if we change f for λf, where λ is some numerical constant. Then, equation 3.1 becomes:

$$\begin{aligned} P(\lambda f) &= C(\lambda f)^{\alpha} \\ &= (C\lambda^{\alpha})f^{\alpha} \end{aligned} \tag{3.2}$$

We observe that the general form of the function is the same as before, i.e. a power law with exponent α. The only thing that changes is the proportionality constant from C to $C\lambda^{\alpha}$. We can therefore "zoom in" or "zoom out" on the function by changing the value of λ while its general shape stays the same. This characteristic gives the signal whose power spectrum follows a power law distribution the property of looking the same under any scale chosen, i.e. the property of scale invariance.

Although scale invariance is an interesting property of fluctuating signals by itself, what is even more interesting is the value of the scaling exponent α, which depends on the correlation properties of the signal. To show this, let us now consider a series of measurements of any given quantity h at discrete times $t_0, t_1, t_2, ...t_N$. This time series, which can also be called signal or noise, can be visualized by plotting $h(t)$ as a function of t.

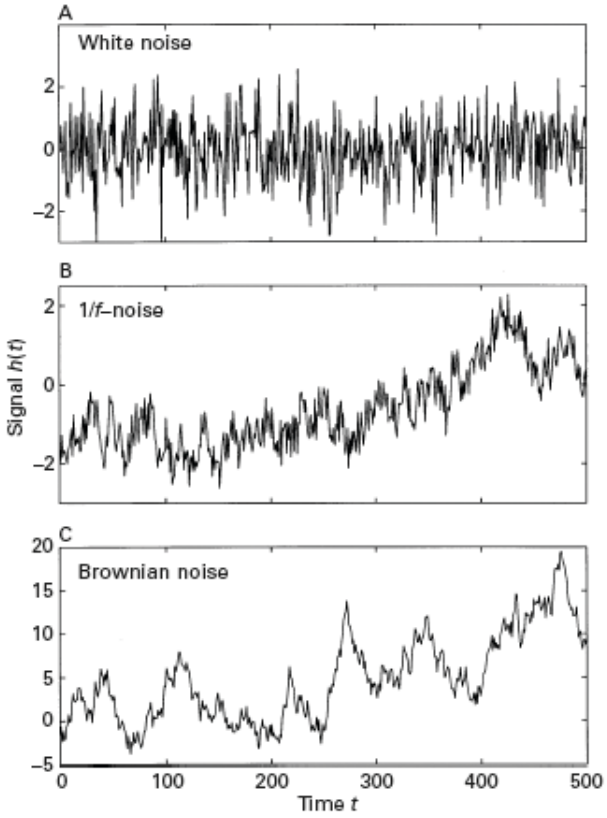

Figure 3.3: Types of noise. Three examples of signals $h(t)$ plotted as functions of time t: white noise (A), $1/f$ - or "pink" noise (B) and Brownian noise (C) (1)

Figure 3.3 shows three types of signals h(t): white noise, "pink" or $1/f$ noise and Brownian noise. The first signal (A) represents a random superposition of waves over a wide range of frequencies. It can be interpreted as a completely uncorrelated signal, meaning that the value of h at a time t is totally independent of its value at any other instant. The third signal (C) represents Brownian noise because it resembles the Brownian motion of a particle in one dimension. This type of signal can be reproduced by what is called a "random walk": the position h of the particle at some time t_n is obtained by adding to its previous position (at time t_{n-1}) a random number representing the thermal effect of the fluid on the particle. Therefore, Brownian noise practically results from the integration of white noise and is considered a strongly correlated signal, as the position of the particle at any given moment totally depends on its previous steps. This is evident by the high content in low frequencies in this signal, that demonstrate a strong "memory" effect.

The second signal (B) is different from the first two, but shares some of their characteristics. It has a tendency towards large variations like the Brownian motion, but it also exhibits high frequencies like white noise. This type of signal seems then to lie somewhere between the two, and is called pink or $1/f$ noise.

Now let us consider the power spectra of the above signals as shown in Figure 3.4. In the case of white noise, which is a superposition of waves of every wavelength, the spectrum should demonstrate equal power $P(f)$ at every frequency f. This could be expressed as:

$$P(f) = f^{\alpha} \tag{3.3}$$

where α is the slope of the line in Figure 3.4 since the power spectrum is expressed in logarithmic axes. An equal distribution of power across frequencies should yield an exponent of $\alpha = 0$, i.e. $P(f) = f^0$, which is indeed the case for the spectrum of white noise where we find a slope of 0.01. The power spectrum of Brownian motion also follows a straight line on a log-log plot with a slope equal to -2 (the line fitted to the signal in Figure 3.4 gives $\alpha = -1.9$), which corresponds to $P(f) = 1/f^2$. The power spectrum of a signal gives a quantitative measure of the importance of each frequency. For Brownian motion, $P(f)$ falls quickly to zero when f goes to infinity, illustrating why $h(t)$ has a small content in high frequencies, making it look smoother compared to white noise. On the contrary the large oscillations, which correspond to low frequencies, constitute the greatest part of the signal.

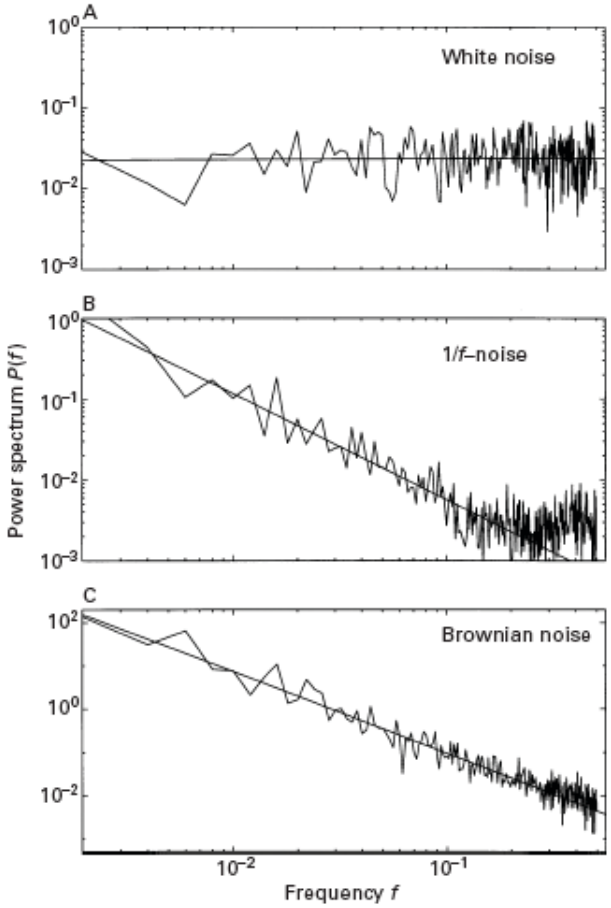

Figure 3.4: Power spectra of distinct types of noise. White noise (A), $1/f$ noise (B) and Brownian noise. The lines fitted to the spectra have slopes of 0.01, -1.31 and -1.9, respectively (1)

Pink or $1/f$ noise is defined by the power spectrum:

$$P(f) = \frac{1}{f} \tag{3.4}$$

which is equivalent to $P(f) = f^{-}1$ with slope -1 or generally within the range $[-0.5, -1.5]$. The interest in $1/f$ noise is motivated by its strong content in both small and large frequencies. $P(f)$ diverges as f goes to zero, which suggests, as in the case of Brownian motion, long-term correlations (or memory) in the signal. In addition, $P(f)$ goes to zero very slowly as f become larger. Pink noise is therefore a signal with a power spectrum without any characteristic frequency or, equivalently, time scale: this

is reminiscent of the notion of fractals, but in time instead of space (1; 29).

Going back to cardiac dynamics, an homeostatic model would consider constant or periodic heart rate patterns as healthy, resulting from efficient control mechanisms which reduce variability arising from external noise. The discovery of fractal, $1/f$ noise in the heart rate spectrum (30), however, suggests that healthy cardiac dynamics should be characterized by complex variability with a significant content in both low and fast frequencies, even in the absence of external stimulation. This intrinsic complex variability permits the heart to rapidly adapt to the continuously changing metabolic requirements dictated either by internal functioning or external factors at different time scales. To illustrate this point, Figure 3.5 shows four heart rate patterns from four different people, only one of whom is healthy. The test consists in identifying the healthy pattern. Guided by an homeostatic principle, one would assume that recordings A and C represent healthy patterns, while B and D seem too erratic and random. Recording B, however, is the only one pertaining to a healthy individual. A and C are from patients in sinus rhythm with severe congestive heart failure and D is from a subject with atrial fibrillation, which produces an erratic heart rate. Recording B shows the type of variability between periodicity and disorganized randomness that is statistically self-similar under many different temporal scales (2).

3.2 Fractal Analysis of Cardiac Dynamics

Detrended Fluctuation Analysis was introduced in 1995 (26) as an algorithm to assess the correlation properties of nonstationary signals. As we have seen, fractal, or self-similar signals, exhibit long-term correlations that extend over many temporal scales. However, physiologic control mechanisms producing fractal signals must be organized in such way that correlations are not that strong and also permit fluctuations at a wide range of scales. This is different from a periodic system with one or a few predominant scales (frequencies). Such a system is considered to be "locked" to a specific mode of functioning and finds it more difficult to adapt to a changing internal or external environment. Fractal correlations also differ from erratic random noise where fluctuations are also present at all scales, but equally distributed. This randomness indicates the absence of any physiologic control and a non-responsive system. Fractal correlations, on the other hand, indicate that all frequencies are present in the signal, but the

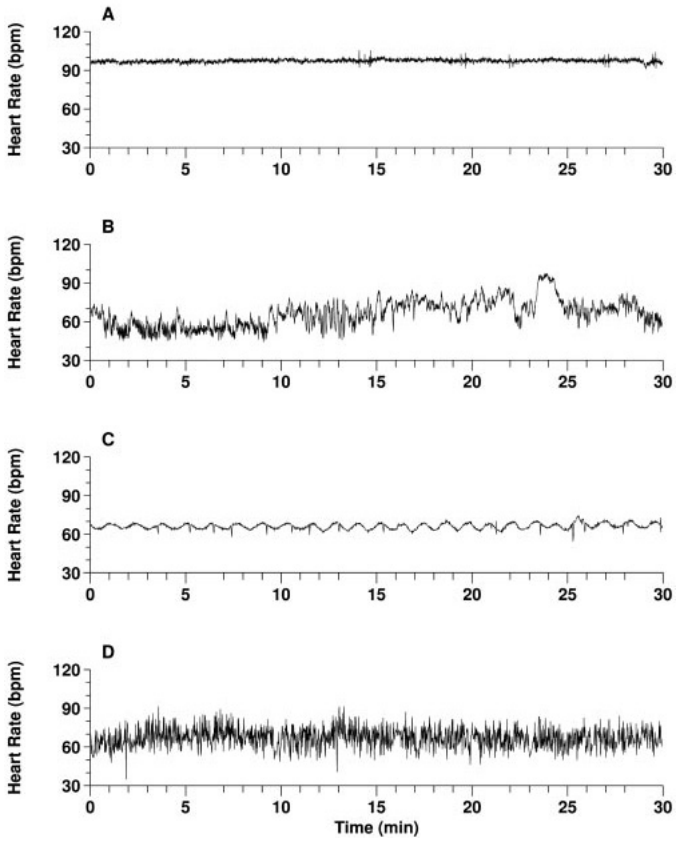

Figure 3.5: Comparing heart rate patterns. Recordings A and C are from patients in sinus rhythm with severe congestive heart failure and D is from a subject with atrial fibrillation, which produces an erratic heart rate. Recording B exhibits fractal variability (2)

distribution of the fluctuations follows an exact power-law that can be evidenced as a straight line with -1 slope in a log-log power spectrum graph. This is why fractal correlation patterns are also known as "$1/f$ noise" (30).

DFA is an algorithm based on the statistical theory of random walk. According to the theory, a walker starting from an initial point in space and making one step at a time towards any direction, will cover a distance depending on time and the correlations between the individual steps. If the direction of each step is decided by a random process, for instance the throw of a dice, the walker will cover a distance of

$$D(s) = cs^{0.5} \tag{3.5}$$

where D is the distance, c a proportionality constant, s the number of steps representing

time, and 0.5 an exponent corresponding to the random correlations in the direction of the steps. If the direction of the steps is correlated (a step towards one direction is more likely to be followed by a step towards the same direction), the exponent will be larger. An exponent of 2 indicates absolute correlation, meaning that the walker moves always towards one direction and covers the maximum possible distance. Values smaller than 0.5 indicate anti-correlations (a step towards one direction is more likely to be followed by a step towards the opposite direction). Fractal correlations give an exponent of 1 and represent a balance between randomness and rigidity (26).

DFA applies the theory of random walk to the heart rate signal in order to assess correlation patterns and explore exponents with values close to 1.0, indicative of scale invariant, fractal variability. The details of the algorithm are presented in the articles presented in chapters five and six. The next chapter presents the software that was developed for the analysis of HRV parameters in this dissertation.

Chapter 4

KARDIA: a Matlab Software for the Analysis of Cardiac Interbeat Intervals

4.1 Introduction

Time intervals between successive heartbeats are obtained from electrocardiographical (ECG) recordings and provide a way to measure heart rate patterns, either in resting states (Heart Rate Variability; HRV) or as response to external stimuli (Phasic Cardiac Responses; PCR). Many commercial data acquisition programs provide algorithms to subtract interbeat intervals (IBIs) from ECG recordings and to calculate some of the most common HRV parameters. The problem of PCR analysis, however, is not addressed by these programs and most researchers depend on custom software to calculate heart rate changes in response to experimental stimuli. In addition, HRV analysis is a field that has gained considerable interest in recent years and a significant number of new metrics deriving from statistical physics have been proposed as complementary to traditional time and frequency domain measures (31). At the same time, older algorithms are continuously being refined, and advanced methods are being tested in order to further improve the assessment of autonomic function in health and disease (32).

As an alternative to commercial software, several free HRV analysis programs are also available to cardiovascular researchers. Two of the most sophisticated and user-friendly are Ecglab (33) and POLYAN (34). Ecglab is a Matlab toolbox that performs

not only HRV analysis, but also R-wave peak detection from raw ECG recordings. HRV analysis functions calculate most common time domain measures, spectral analysis parameters and also present time-frequency graphs and metrics. Importantly, its open source philosophy allows users to modify the existing algorithms according to their specific needs. POLYAN is another open source Matlab software designed for the simultaneous analysis of several recording signals for the assessment of autonomic regulation. Its HRV analysis algorithms calculate both time and frequency domain metrics and provide elaborate graphs that facilitate the understanding and interpretation of numerical results. Another useful, and freely available HRV analysis program (35), also provides common estimates of time and frequency domain measures.

In this article we present KARDIA ("heart" in Greek), a Matlab software designed for the analysis of PCRs and HRV. Kardia is an open source project hosted by sourceforge, which means that it is subjected to continuous development by an increasing number of researchers (36). Its main advantage compared to the programs presented above is its capacity for simultaneous analysis of multiple datasets, calculation of grand average statistics across subjects and experimental conditions and generation of analytic spreadsheets that can be directly subjected to further statistical analysis by related software.

Furthermore, KARDIA performs PCR analysis based on event codes corresponding to external stimuli presented under specific experimental conditions. These phasic responses are calculated by coherent averaging which provides a valid estimation of event-related changes as unrelated fluctuations are cancelled out. Results are compared to a baseline period prior to the stimulation where nonspecific fluctuations are expected (37). The assessment of phasic heart rate responses is a fundamental index of emotional modulation during affective picture processing (38) or an important measure of orienting and attention (39), just to cite two examples.

4.2 Program Description

KARDIA is intended to be a useful tool for researchers with no specific programming skills and therefore all functionalities are directly available from an intuitive graphical user interface (GUI).

PCRs time-locked to specific events may be calculated using either weighted averages or a range of interpolation methods. Common time and frequency domain HRV statistics are also estimated. The power spectrum is calculated using either fast Fourier transform or parametric methods, and scaling exponents of IBI fluctuations are computed using DFA (26). Individual subject results and grand average statistics can also be exported to Excel spreadsheets for further statistical analysis.

KARDIA was entirely written in Matlab scripting language. All functions are contained within a single m-file (*kardia.m*), although the complete software package includes the software logo, a matrix with GUI-related information, documentation and sample data stored in different subfolders. The open access policy, guaranteed through the General Public License (GPL), allows more experienced users to adapt the code to address their own specific needs.

4.2.1 The graphical user interface

KARDIA's GUI is divided into four different panels (Figure 4.1): the load data and event information panel (top-left), the PCR analysis panel (bottom-left), the HRV analysis panel (center) and the results panel (right). The interface allows the user to load several data files simultaneously, manually set the analysis parameters and plot graphs of the results. A toolbar with four icon buttons at the top of the main window offers direct access to specific functionalities, such as save as, export to and help.

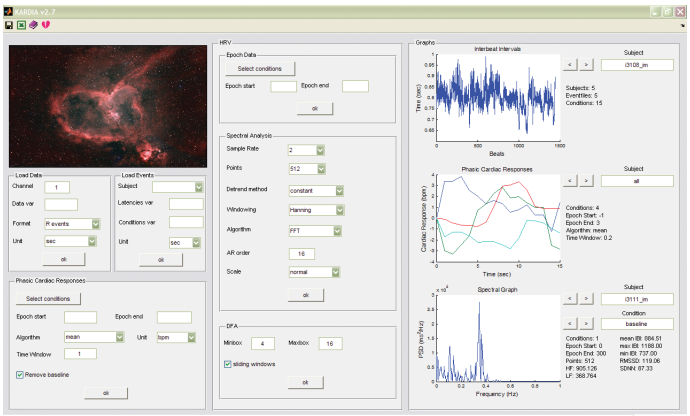

Figure 4.1: The graphical user interface of KARDIA

4.2.1.1 Load IBI data and event information panel

IBI data must be provided as a numeric vector saved in a Matlab mat-file. Data from several subjects may be imported simultaneously from different mat-files for analysis. Working with mat-files guarantees compatibility with almost all R-wave detection programs since there are many freely available algorithms that convert from almost any file format to Matlab mat-file. The IBI data vectors can either be in the form of time intervals between adjacent R-waves (IBI series) or R-wave peak times relative to the beginning of the recording (the cumulative sum of IBI series).

Event-related information for each subject needs to be saved in separate mat-files. An event is defined by its *onset time* in seconds or milliseconds from the beginning of the recording together with an identifying *code* specific to the type of the event. Onset times are saved as a numeric vector and the codes are stored in a cell structure as string variables. Hence, every event file must include two different variables of the same length: the onset time variable and the event codes variable. According to the experimental design the same event structure can be used for all subjects or different event files can be imported and matched with each subject's dataset. In the latter case, different event structures must be imported individually for each subject.

4.2.1.2 PCR analysis panel

The first step in performing PCR analysis is to select the events (conditions) that should be averaged. The user then needs to define a baseline period, before the event's onset as well as the event's duration. A drop-down menu offers a choice of algorithms that can be used to calculate the heart rate changes during the event: "mean", "CDR", "constant", "linear" and "spline".

The "mean" algorithm applies the *fractional cycle counts* method described in (40) whereby every IBI $[t_0, t_1], [t_1, t_2]$ is taken as a cardiac cycle. For an analysis window with onset time at T_0 and duration $T_1 - T_0$ the number of cycles within the window $[T_0, T_1]$ is counted. Cycle $[t_{i-1}, t_i]$ is counted as one if $T_0 \leq t_{i-1} < t_i \leq T_1$, as $(t_i - T_0)/(t_i - t_{i-1})$ if $t_{i-1} < T_0 < t_i \leq T_1$, as $(T_1 - t_{i-1})/(t_i - t_{i-1})$ if $T_0 \leq t_{i-1} < T_1 < t_i$ and as $(T_1 - T_0)/(t_i - t_{i-1})$ if $t_{i-1} < T_0 < T_1 < t_i$. Having defined the cycle count within a window, the mean heart rate is given by the ratio of this count to the total window length (40). Reyes del Paso and Vila (41) showed that this fractional counting procedure

is equivalent to the weighted averages method proposed by Graham in 1978 (42) which is the standard procedure used in psychophysiological research.

The algorithm "CDR" can be used to calculate the Cardiac Defense Response, according to the paradigm established by Vila et al (43). The heart response elicited by an intense auditory stimulus is calculated during 80 seconds after the onset of the stimulus and is expressed in terms of second-by-second heart rate changes compared to a baseline of 15 seconds prior to the presentation of the stimulus. These second-by-second heart rate values are subsequently averaged across a group of participants based on 10 points corresponding to the medians of 10 progressively longer intervals: 2 of 3 sec, 2 of 5 sec, 3 of 7 sec and 3 of 13 sec. This simplified representation facilitates statistical analysis without altering the topographic characteristics of the response (43).

KARDIA also includes algorithms to calculate instantaneous heart rate at a sample rate defined by the user using a choice of three different interpolation methods: "constant, "linear or "spline interpolation. The "constant" method assigns the same value to every point between two IBIs. The "linear" method interpolates two adjacent IBIs with a straight line and the "spline" method uses a cubic spline function to interpolate the IBI series.

The user is further required to define the analysis window duration for the "mean" method, or the sample rate for the interpolation algorithms. The option also exists to calculate the heart period instead of heart rate changes and wether or not to subtract the baseline heart rate (or heart period) value when graphically representing the results. When all parameters are set, the program plots a grand average across all subjects for the selected conditions as well as individual graphs for each subject. Clicking on any of KARDIA's embedded graphs opens a new figure with the same plot that can be processed and saved in the same way as ordinary Matlab figures.

4.2.1.3 HRV analysis panel

HRV analysis is performed on a single epoch over the entire IBI series. The user is asked to select one event code and set the epoch's start and end time relative to the onset of the selected event.

Spectral analysis

Spectral analysis of HRV is used for the assessment of the variance of IBI fluctuations in specific frequency bands that correspond to identifiable physiological processes such as the vagally-mediated respiratory sinus arrhythmia (RSA) and the baroreflex. As a first step, the IBI series is interpolated by cubic splines at a user-defined sample rate (2 or 4 Hz). The interpolated series is subsequently detrended, either by removing the best straight-line fit, or by subtracting the mean value. Next, the signal is multiplied by a window function (Hanning, Hamming, Blackman or Bartlett) to reduce artifacts on the frequency spectrum due to signal truncation. The Discrete Fourier Transform (DFT) is calculated by means of Fast Fourier Transform (FFT) algorithm for a number of points defined by the user (the FFT algorithm requires that the number of data points is a power of 2). The Fourier power spectral density (PSD) is then obtained from the squared absolute value of the DFT which is multiplied by the sampling period and divided by the number of samples in the signal. In addition, a coefficient described in (44) is used to remove the effect of the window function from the total signal power.

Alternatively, Matlab's arburg function that uses Burg method to fit an autoregressive (AR) model of variable order to the IBI signal, can be applied (45). The power spectrum is then calculated from the squared absolute value of the AR system parameters, multiplied by the sample period and the variance of the white noise input to the AR model.

By default, the frequency spectrum is divided into 3 bands: VLF (0 to 0.04 Hz), LF (0.04 to 0.15 Hz) and HF (0.15 to 0.5 Hz). It is relatively easy, however, to modify these settings in the relevant part of the program code in *kardia.m*. The area under the PSD curve represents the statistical variance and is calculated separately for each frequency band by means of numerical integration. KARDIA graphically represents the PSD for each subject and condition together with key time domain statistics and the HF and LF variance.

Detrended fluctuation analysis

DFA is an algorithm introduced by Peng (26) that has proven to be very successful in quantifying the correlation properties of nonstationary time series derived from biological, physical and social systems. DFA has been applied to diverse research fields such as economics (46), climate change (47), DNA (48), neural networks (49) and cardiac dynamics (26). In its application to HRV, the IBI series (of length N) is first

integrated, to calculate the sum of the differences between the ith interbeat interval $B(i)$ and the mean interbeat interval $\overline{B}$: $y(k) = \sum_{i=1}^{k}[B(i) - \overline{B}]$. Next, the integrated series $y(k)$ is divided into boxes of equal length n (measured in number of beats). Each box is subsequently detrended by subtracting a least-squares linear fit, denoted $y_n(k)$. The root-mean-square (RMS) fluctuation of this integrated and detrended time series is calculated by

$$F(n) = \sqrt{\frac{1}{N}\sum_{k=1}^{N}[y(k) - y_n(k)]^2} \tag{4.1}$$

The algorithm is then repeated over a range of box sizes to provide a relationship between the average fluctuation $F(n)$ as a function of box size n. Normally, $F(n)$ will increase as box size n becomes bigger. A linear relationship on a log-log graph indicates the presence of fractal scaling whose exponent is given by the gradient (usually referred to as the α exponent). For uncorrelated time series (white noise), the integrated $y(k)$ is a random walk, which yields an exponent of $\alpha = 0.5$. A scaling exponent larger than 0.5 indicates the presence of positive correlations in the original time series such that a large IBI is more likely to be followed by another large interval, while $0 < \alpha < 0.5$ indicates anti-correlations such that large and small IBI values are more likely to alternate. The special case of $\alpha = 1.5$ is obtained by the integration of highly correlated *Brown* noise, while $\alpha = 1$ corresponds to $1/f$ noise that reflects a balance between the step by step unpredictability of random signals and highly-correlated Brownian noise (50).

KARDIA allows the user to define the minimum and maximum box size for the DFA analysis and whether or not to implement a sliding windows (overlapping) version of the algorithm which increases precision, but is computationally more intensive.

4.2.1.4 Results panel

KARDIA's results panel is further divided into three sub-panels. The top sub-panel provides information on the number of subjects, event files and conditions imported. After importing data, the IBI series for each subject are plotted in this sub-panel. Users can use the arrow buttons to scroll through subjects or type the name of a subject to directly see their IBI plot.

The second sub-panel corresponds to the PCR analysis. At any given moment, users can see the conditions selected, the algorithm used as well as the analysis window

defined. The graph plots the grand average for each condition, but also allows the user to inspect individual subject's results through the use of the arrows buttons.

The third sub-panel presents the results of the HRV analysis. HRV statistics are instantly updated each time the user runs a new analysis of the data. The graph plots the power spectrum and the DFA graphs for each subject and condition. Once again, users can scroll through subjects by using the arrows or by typing the name of the target subject. The same is also true for differing conditions.

4.2.1.5 Toolbar buttons

The first toolbar button allows the user to save a mat-file in the current directory containing all the data and event information imported into KARDIA, as well as all the parameter settings relevant to the current analysis. This allows a previously ongoing analysis to be resumed and all the required information, including data and parameter settings, to be saved in a single file thus facilitating data sharing.

The second toolbar button is used to export the numerical results of the last analysis performed (PCR and HRV) to an excel file. The excel spreadsheet generated contains five different tabs: a "General" tab with information about subjects and events, a "PCR" tab with the heart rate (or heart period) estimates for each subject and condition, a "Grand Average PCR" tab with the grand average results for PCR analysis, an "HRV" tab with the measures of all subjects and conditions, and a "Grand Average HRV" tab with the grand average HRV statistics.

The last two toolbar buttons are for launching the "User's Guide" in pdf format and for opening a dialog window displaying the program's copyright agreement, respectively.

4.2.2 System requirements

KARDIA requires less than 1 MB of free hard disk space. The program will run on any operating system supporting Matlab 7.0 (The MathWorks Inc., MA) or later that has the Matlab Signal Processing Toolbox (The MathWorks Inc., MA) installed. The program's current version (v.2.7) has been tested in Matlab R2007b on Mac OS X, version 10.5 (Apple Inc., CA), Ubuntu 8.10 Linux, and Microsoft Windows XP (Microsoft Inc., WA).

4.2.3 Installation Procedure

After downloading and unzipping the KARDIA package, the only step that needs to be followed is to add the package's folder and subfolders to Matlab's path.

4.2.4 Availability

KARDIA is distributed free of charge under the terms of the GNU General Public License as published by the Free Software Foundation (51). Users are free to redistribute and modify it under the terms of the GNU license. KARDIA is freely available for download at http://sourceforge.net/projects/mykardia/.

4.3 Sample runs

KARDIA's PCR module was tested on IBI data obtained from 24 subjects (15 female; 21 yrs ± 1.7) in a picture viewing paradigm. "Neutral" images (people) and "unpleasant" images (mutilated bodies) drawn from the International Affective Picture System (52) were presented to the subjects on a computer screen while continuous ECG was being recorded. Each picture presentation trial was initiated with a fixation cross lasting from 500 to 900 ms. The picture (neutral or unpleasant) was subsequently presented during 200 ms. A checkerboard mask was then projected during 3 sec, until the beginning of the next trial. ECG was recorded from a bipolar chest lead, filtered with a high pass filter (0.5 Hz cutoff frequency) and sampled at 240 Hz. R-wave detection and artifact correction were performed with Ecglab (33).

IBI data for all 24 subjects was imported into KARDIA together with an event file for each subject containing the onsets of the two types of events (neutral and unpleasant picture presentation). In the PCR panel we first chose to analyze both conditions (neutral and unpleasant) and then selected -0.5 sec for "epoch start" and 3 sec for "epoch end" boxes. The program then uses a 500 ms period before stimulus onset to obtain the baseline heart rate and calculates heart rate changes compared to this baseline value for 3 sec post-stimulus. We selected the "mean" option to implement a weighted averages algorithm, "bpm" to obtain the results in heart rate instead of heart period as well as the value 0.2 for the "Time window" to calculate a weighted average heart rate value every 200 ms. We also checked the "Remove baseline" box to

plot heart rate changes against the baseline instead of absolute heart rate values in the results graph.

Figure 4.2 shows the result of the PCR analysis for the selected parameters as it appears in KARDIA's results panel. The grand average over all subjects is first plotted, but users can use the arrows to scroll through the results for individual subjects. A potentiated bradycardia is observed in the unpleasant picture condition (blue line) compared to control (green line), as expected according to the literature on the orienting reflex in humans (53). The embedded graph does not include a legend, but clicking it with the mouse left-button opens the same plot in a new figure window that includes a legend and can be editted and saved in various formats.

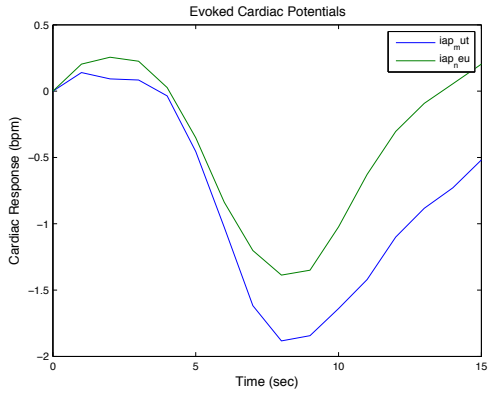

Figure 4.2: The PCR results panel. The grand average over all subjects indicates a potentiated bradycardia in the unpleasant picture condition (blue line) compared to control (green line)

The HRV module was tested comparing a 5 min resting period before and after atropine administration. First, in HRV's "Epoch Data" panel, we chose the event code named "before drug" and set "Epoch start" to 0 and "Epoch end" to 300. This defined a specific epoch on the entire IBI record whose onset coincided with the event code named "before drug" (time 0) and lasting 5 min (300 sec). Right after epoch selection, the selected IBI epochs for each subject are displayed in the HRV sub-panel of the results panel. The next step was to select the spectral analysis parameters in the corresponding panel. For this example we selected the default values: 2 Hz for the sampling rate, 512 points for the DFT, a "constant" detrending method, Hanning as the window function

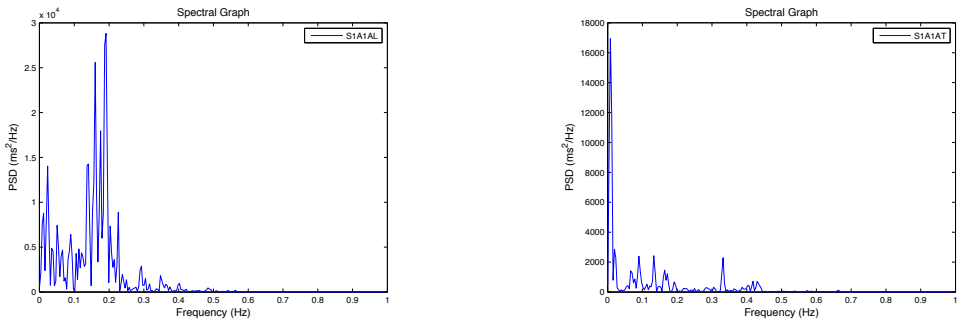

(a) Before Atropine

(b) After Atropine

Figure 4.3: The HRV results panel. Figure 4.3(a) shows the spectral graph of a 5 min segment before atropine administration. In Figure 4.3(b), which presents a spectral graph for the same subject after atropine administration, we observe the elimination of respiratory-related oscillations due to parasympathetic blockade

and FFT for spectral estimation. We repeated the same procedure choosing the label "after drug" as the event code in the "Epoch Data" panel. Figure 4.3 presents a comparison between the two conditions. The absence of respiratory-related oscillations due to parasympathetic blockade is obvious in the second condition. Once again users can scroll through subjects to quickly review snapshots of individual spectrograms and statistics.

Finally, the Excel toolbar button can be used to save a specially-formated excel file with the results from all analyses (PCR and HRV) performed. This file provides grand average as well as individual statistics that are then amenable to further processing with statistical packages like R, SPSS etc.

4.4 Conclusion

KARDIA is currently in use by research laboratories at Harvard Medical School and Boston University in the USA, at the Universities of Granada and Castellon in Spain, and at the Federal University of Rio de Janeiro in Brasil. It has proven to be very useful in a variety of psychophysiological experiments. Experienced and inexperienced researchers have profited from its graphical user interface, reporting improved analysis time and ease of data manipulation.

4. KARDIA: A MATLAB SOFTWARE FOR THE ANALYSIS OF CARDIAC INTERBEAT INTERVALS

One of KARDIA's main advantages over other available software for IBI analysis is its ability to load data from many subjects simultaneously through the GUI and to calculate grand average PCRs and HRV statistics across all subjects. In addition, the program saves all information about imported datasets and numerical results in a single "mat" file that substitutes the numerous IBI and event information files and facilitates data storage and sharing.

KARDIA is being actively maintained and developed. New functionality is expected to be included in future versions, such as algorithms for automatic IBI artifact detection and nonlinear HRV analysis.

Chapter 5

Breathing Frequency Bias in Fractal Analysis of Heart Rate Variability

5.1 Introduction

Extraordinary structural and functional complexity is a defining characteristic of living organisms. This complexity gives rise to physiological signals that exhibit interesting properties such as scale invariance and long-term correlations. Statistical physics has only recently began to develop the appropriate mathematical tools to understand and quantify these properties present in a wide variety of biological, physical and social complex systems (54; 55; 56).

Generally, signals exhibiting fluctuations whose distribution obeys a power law over a broad range of frequencies are scale invariant and usually referred to as fractal (23). Fluctuations (F) in these signals can be expressed as a function of the time interval (n) over which they are observed according to the formula:

$$F(n) = pn^{\alpha} \tag{5.1}$$

where p is a constant of proportionality and α is a scaling exponent that depends on the signal correlation properties. The special case of $\alpha = 1$ is frequently observed in nature and is often called $1/f$ *noise*. Signals exhibiting $1/f$ noise are characteristic of complex dynamical systems, composed of multiple interconnected elements and

functioning in far from equilibrium conditions (57). These systems demonstrate optimal stability, information transmission, informational storage and computational power (58). Hence, $1/f$ fluctuations are commonly considered as an indicator of the efficacy and adaptability of the system that produces them (59).

HRV has been extensively studied by psychophysiologists as an indirect index of autonomic function in health and disease (32; 60). Common HRV measures include time and frequency domain metrics. Time domain measures calculate the overall variance or the variability between successive interbeat intervals (IBI) using linear statistics. Frequency domain measures assess the variability of the power spectrum in predetermined frequency bands. The rationale for the use of all these different HRV methods in psychophysiological research is to identify and measure characteristic components of heart rate fluctuations that can be associated with specific physiological control mechanisms such as respiratory sinus arrhythmia (RSA) and baroreflex activity (61).

The power spectrum of 24-hr heart rate records, however, also reveals that the proportion of the signal in different frequency bands is inversely proportional to the frequency over a wide range of scales (30; 62). This evidence of fractal $1/f$ noise in heart rate fluctuations may imply that cardiac regulation mechanisms are organized in a critical state that allows maximum adaptability to internal and external stimulation (55). More detailed aspects of this organization can be assessed by algorithms that preserve the temporal information present in the signal. DFA is one of the algorithms that has been widely used to quantify IBI correlation properties as a complementary measure to more traditional HRV indices (63; 64). Initial results indicate that healthy HRV is characterized by $1/f$ scaling, while deviations from this value are associated with aging and disease (65; 66).

The aim of this study is twofold. Firstly, to introduce in a brief and concise manner the DFA as an HRV measure that is rarely encountered in the biopsychological literature. We believe that scaling analysis of cardiac dynamics can be used effectively to probe how complexity is generated in the cardiovascular system and also to improve our understanding of how the heart responds to internal and external stimulation. With this in mind, in the discussion section we include some specific suggestions for further research. Our second objective is to call attention to an important methodological issue in the fractal analysis of short-term HRV that has not been properly addressed in

the literature. In our concluding remarks we will articulate our opinion regarding the delicate issue of applying the DFA on short-term HRV.

5.1.1 Detrended Fluctuation Analysis

DFA was introduced by Peng (26) and has been successfully used to quantify correlation properties in nonstationary time series derived from biological, physical, and social systems. It has been applied in various research fields including economics (46), climate temperature fluctuations (47), DNA (48), neural networks (49), and cardiac dynamics (26). In the application of DFA to HRV, the IBI series B (of length N) is first integrated in order to calculate the sum of the differences between the ith interbeat interval $B(i)$ and the mean interbeat interval B_{ave}: $y(k) = \sum_{i=1}^{k}[B(i) - B_{ave}]$. Next, the integrated series $y(k)$ is divided into boxes of equal length n (measured in number of beats). Each box is subsequently detrended by subtracting a least-squares linear fit, denoted $y_n(k)$. The root-mean-square (RMS) F of this integrated and detrended time series is calculated by

$$F(n) = \sqrt{\frac{1}{N}\sum_{k=1}^{N}[y(k) - y_n(k)]^2} \tag{5.2}$$

This algorithm is repeated over a range of box sizes to provide a relationship between the mean fluctuation $F(n)$ as a function of box size n. Normally, $F(n)$ will increase as box size n becomes larger. According to equation 5.1, a linear relationship on a log-log graph indicates the presence of scaling characterized by the scaling exponent α. For uncorrelated time series (white noise), the integrated $y(k)$ is a random walk that yields an exponent of $\alpha = 0.5$. A scaling exponent $\alpha > 0.5$ indicates the presence of correlations in the original series such that a large IBI is more likely to be followed by another large interval, while $0 < \alpha < 0.5$ indicates anti-correlations such that large and small IBI values are more likely to alternate. The special case $\alpha = 1.5$ is obtained by the integration of highly correlated *Brown* noise and $\alpha = 1$ corresponds to $1/f$ noise which can be interpreted as a balance between the complete step-by-step unpredictability of random signals and highly-correlated Brownian noise (50).

5.1.2 Application to IBI records

Peng et al (26) applied the DFA algorithm to 24-hr IBI records obtained from healthy subjects and patients with congestive heart failure, revealing two distinct scaling regions

for both groups: one corresponding to short-term variability (smaller box sizes) and the other associated with long-term variability (larger box sizes). Therefore two different scaling exponents were obtained: a short-term exponent for $4 \leq n \leq 16$ referred to as α_1 and a long-term exponent for $n \geq 16$ referred to as α_2.

Figure 5.1 plots log $F(n)$ against log n (which we will refer to as the DFA plot) for two subjects from the same database, which is freely available from the Physionet website (67). It shows the two distinct scaling regions and their corresponding slopes. The arrows indicate the box size where the scaling changes (the crossover point). In healthy subjects, $1/f$ noise represented by $\alpha_2 \approx 1$ is exhibited over a broad range of time scales from mid to low frequencies (from $n = 16$ to $n = 3400$). Stronger correlations are found at higher frequencies (from $n = 4$ to $n = 16$), reflected by $\alpha_1 > 1$. In patients with congestive heart disease, long-term variability loses its fractal $1/f$ properties ($\alpha_2 > 1$), while short-term variability approximates uncorrelated randomness ($\alpha_1 \approx 0.5$).

5.1.3 Effects of sinusoidal trends on DFA

As noted above, scaling behavior is not constant throughout the IBI series, with crossovers occurring at the changeover from one RMS fluctuation power law to another. A crossover can arise either from a change in intrinsic IBI correlation properties or from external trends in the data (26). Therefore, a correct interpretation of the scaling exponent is necessary to distinguish between intrinsic heart rate fluctuations and trend-like fluctuations arising from other systematic effects. Distinctions of this kind are relevant because strong trends in the data can lead to a false detection of long-range correlations if DFA results are not carefully interpreted (68; 69).

The DFA algorithm is capable of identifying and removing both linear and higher-order polynomial trends and avoids the spurious detection of apparent long-range correlations (68). However, this is not the case for exponential or sinusoidal trends (70; 71). In Figure 5.2 we present the DFA plot of correlated noise with scaling exponent $\alpha = 0.8$, superimposed by a sinusoidal trend with period $T = 15$ samples. The same graph also includes the DFA plot for the noise and sinusoidal trend separately. Constant scaling is observed with $\alpha \approx 0.8$ for the noise. However, the sinusoidal trend shows a clear crossover n_x, dividing $F(n)$ into two very distinct scaling regions. Hu et al (69) showed that this crossover is found at a scale corresponding to the period of the sinusoid and is independent of its amplitude. For $n < n_x$, integration of the sinusoid produces a

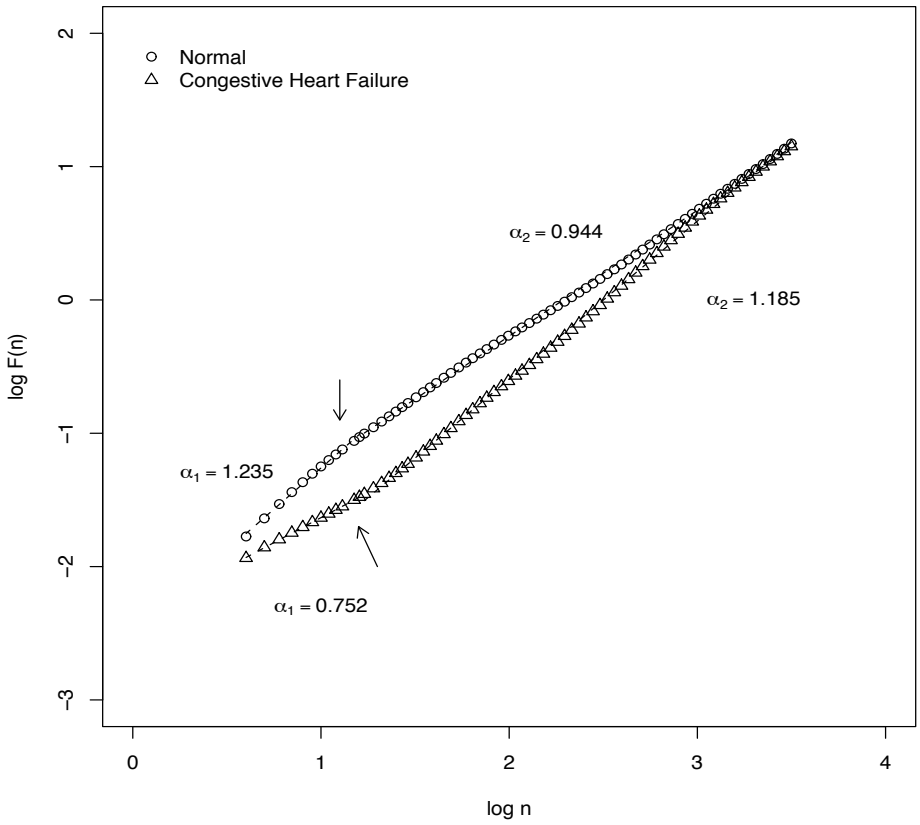

Figure 5.1: Plot of $\log F(n)$ vs. $\log n$ from a healthy subject (circles) and from a subject with congestive heart failure (triangles). Arrows indicate crossovers that divide the DFA plot into two distinct scaling regions

quadratic background that is not filtered out by the linear detrending of the DFA algorithm. Thus, in this region, $F(n)$ is sensitive to the quadratic trend and the slope of log $F(n)$ increases steeply as box sizes become larger. For $n > n_x$, the box size is large enough to contain a whole cycle and, at these scales, fluctuations associated with local gradient changes along the sine wave are not detectable. Hence, $F(n)$ no longer depends on n, leading to a flattening of the DFA plot.

The DFA plot of the noise and sinusoidal trend shows a scaling behavior produced by competition between the two signals. To explain this effect analytically, Hu et al demonstrated that for any two independent signals ($s1$ and $s2$), the RMS fluctuation function for a third signal resulting from their superposition is given by

$$[F_{s1s2}(n)]^2 = [F_{s1}(n)]^2 + [F_{s2}(n)]^2 \tag{5.3}$$

This "superposition rule" allows a mathematical description of how the competition between the contribution of the fluctuation function of the correlated noise $F_{noise}(n)$ and the fluctuation function of the sinusoidal trend $F_{sinus}(n)$ at different scales n leads to the appearance of scaling crossovers (69). For $n < n_x$, $F_{sinus}(n)$ is dominant, leading to a high DFA exponent ($\alpha = 1.328$). For $n > n_x$, however, the contribution of $F_{noise}(n)$ increases, leading to a gradual decrease in the DFA exponent.

At high frequencies, HRV is dominated by rather smooth rhythmical oscillations associated with breathing (RSA) (72). In the IBI power spectrum of healthy individuals at rest, RSA is evidenced as a clearly distinct peak at the respiratory frequency (3). We assumed therefore that RSA would produce a scaling behavior of short-term HRV similar to that of a sinusoidal trend superimposed on correlated noise. It can be argued that RSA is not always adequately approximated by a sinusoid since there is significant variability in the inspiration/expiration ratio (73). However, it is clear from our previous analysis that the strongly correlated region at scales smaller than the crossover is caused by increases in the fluctuation function $F(n)$ that are mostly influenced by the local constant gradient of the periodic signal and not by the exact form of the sinusoidal function.

To experimentally test the above assumption, we designed a study to explore the effects of RSA on the DFA of IBI series and compared them with those observed when a sinusoidal trend is superimposed on a correlated noise. We proposed two hypotheses:

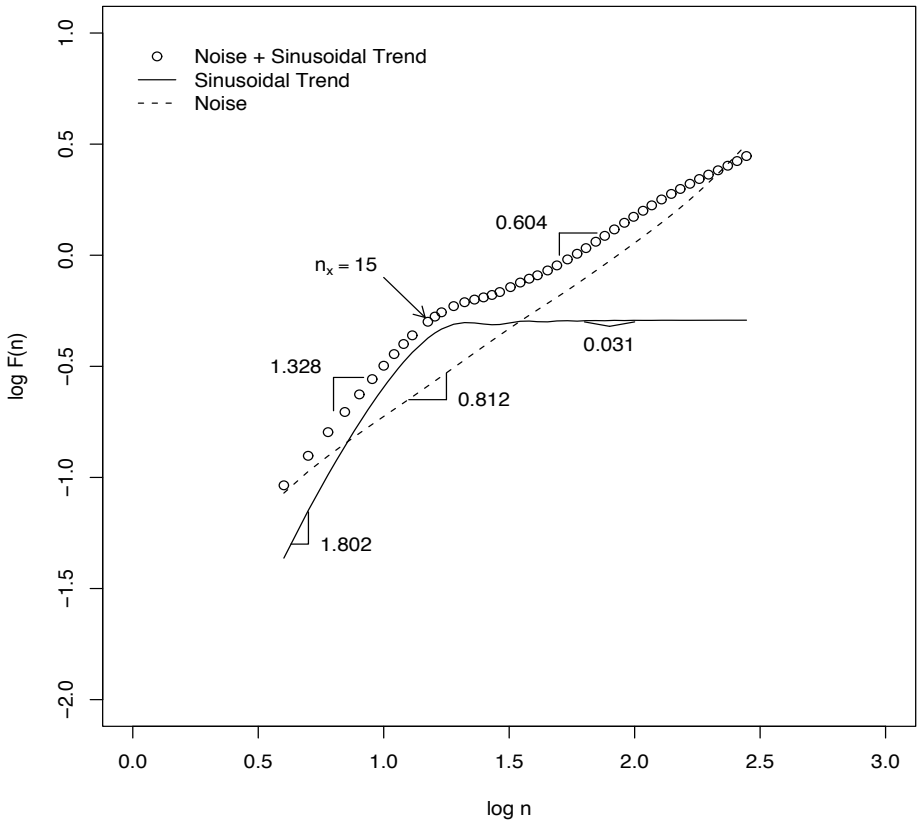

Figure 5.2: Crossover behavior of the fluctuation function $F(n)$ for correlated noise superimposed with a sinusoidal function with period $T = 15$. The fluctuation function for noise and the fluctuation function for the sinusoidal trend are shown separately for comparison. The arrow indicates the scaling crossover at scale $n_x = 15$ ($log_{10}(15) = 1.1761$) corresponding to the period of the sinusoidal trend

1. Respiratory oscillations produce a crossover that divides the log $F(n)$ plot into two significantly different scaling regions.

2. Changes in breathing frequency $B(f)$ affect the location of the crossover, producing predictable alterations in the value of the short-term scaling exponent obtained by the DFA algorithm.

5.2 Method

The hypotheses were tested in a physiological experiment involving 14 university students (6 male) aged $20 - 23$ yrs ($mean = 21.79 \pm 0.89$ yrs), who were instructed to breathe at specific frequencies (0.1Hz, 0.2Hz and 0.25Hz) following a sinusoidal tone heard on headphones. Each breathing condition lasted for five minutes and was preceded by a training session to ensure participants were able to perform the task without difficulties. At the end of each breathing condition, subjects were given the chance to have a short break to relax before commencing with the next respiratory pattern. Prior to the three breathing conditions, that were always performed in the same order, we also recorded five minutes of spontaneous breathing. During each experimental session, continuous ECG (at a sample rate of 1000 Hz) was recorded by a Powerlab data acquisition system ($4/25T$). R-wave detection and artifact correction were performed with *Ecglab* (33).

The location of the crossover in the plot of log $F(n)$ was calculated for each subject using the relation,

$$n_x = \frac{T}{< IBI >} \tag{5.4}$$

where T is the respiratory period and $< IBI >$ is the average heart period calculated over the entire 5-min breathing period. Equation 5.4 therefore represents the box size (number of beats) that contains a complete respiratory cycle dependent on the average interbeat interval of each subject.

KARDIA (74), a Matlab Toolbox designed for IBI data analysis was used to obtain scaling exponents, power spectrum graphs and DFA plots. Spectral analysis was performed after interpolating the IBI series with cubic splines at 2Hz. The interpolated series was subsequently detrended, by removing the best straight-line fit and multiplied by a Hanning window function. The discrete Fourier transform (DFT) was calculated

by means of fast Fourier transform with 512 points. Finally, the Fourier power spectral density was obtained from the squared absolute value of the DFT, multiplied by the sampling period and divided by the number of samples in the signal. The short-term DFA exponent was calculated after implementing a first-order DFA algorithm (as described in section 1.2) for box sizes ranging from 4 to 16 beats according to the original suggestion by Peng et al (26). To avoid ambiguity, the designation α_{4-16} was selected for this short-term DFA exponent, which is usually denoted α_1 in the literature, because we will use the terms α_1 and α_2 to refer to the exponents of the two scaling regions defined by the respiratory crossover. Statistical significance was tested by paired Student's t-test.

5.3 Results

Visual inspection of the power spectra revealed distinctive peaks at the expected frequencies (0.1, 0.2 and 0.25 Hz) for all subjects and conditions. This was used as a measure to assure that participants had followed the instructions correctly producing the desired respiratory patterns. Table 5.1 shows the average IBI values, the predicted box size at which the respiratory crossover should appear according to equation 5.4, the scaling exponent for the two regions defined by the crossover, and the scaling exponent obtained for $4 \leq n \leq 16$.

To test our first hypothesis, we compared the scaling exponents obtained for the regions before and after the location of the respiratory crossover (α_1 and α_2 respectively). In all breathing conditions, the two exponents were significantly different, confirming the hypothesis. In every case, α_1 was significantly higher than α_2 ($Bf = 0.1$ Hz: $t_{13} = 23.21$, $p < 0.001$; $Bf = 0.2$ Hz: $t_{13} = 16.65$, $p < 0.001$; $Bf = 0.25$ Hz: $t_6 = 7.77$, $p < 0.001$[1]).

Our second hypothesis was tested by examining the effect of breathing frequency on the α_{4-16} exponent. We found that α_{4-16} was significantly reduced when the breathing frequency was increased from 0.1 to 0.2 Hz ($t_{13} = 11.59$, $p < 0.001$). The comparison of α_{4-16} at 0.2 and 0.25 Hz revealed no significant differences ($p = 0.487$). The high α_1 exponents in all breathing conditions are illustrated in the DFA plots for one subject

[1]For $Bf = 0.25$ Hz, the α_1 exponent could only be calculated for the cases in which $n_x > 4$.

Table 5.1: Results for 14 subjects breathing at frequencies of 0.1, 0.2, and 0.25 Hz. IBI is the average cardiac interbeat interval, n_x is the predicted scale of the respiratory crossover, α_1 and α_2 are the exponents for the two scaling regions defined by the crossover, and α_{4-16} is the exponent for the region from 4 to 16 beats. There are data gaps at 0.25 Hz due to the small value of n_x in the fast breathing condition.

	0.1 Hz					0.2 Hz					0.25 Hz				
Subjects	IBI	n_x	α_1	α_2	α_{4-16}	IBI	n_x	α_1	α_2	α_{4-16}	IBI	n_x	α_1	α_2	α_{4-16}
1	823	12	1.628	0.528	1.41	818	6	1.496	0.668	0.86	831	4		0.881	0.92
2	945	10	1.636	0.364	1.23	958	5	1.456	0.493	0.64	983	4		0.399	0.44
3	785	12	1.594	0.722	1.42	763	6	1.336	0.848	0.98	770	5	1.521	1.07	1.13
4	801	12	1.469	0.562	1.29	810	6	1.429	0.589	0.8	852	4		0.482	0.55
5	820	12	1.52	0.534	1.33	818	6	1.4	0.285	0.58	808	4		0.599	0.66
6	917	10	1.678	0.428	1.28	913	5	1.582	0.822	0.95	908	4		0.845	0.88
7	808	12	1.655	0.545	1.44	813	6	1.515	0.365	0.67	817	4		0.812	0.87
8	734	13	1.552	0.65	1.43	714	7	1.426	0.629	0.89	714	5	1.642	1.222	1.29
9	763	13	1.597	0.68	1.46	751	6	1.677	1.086	1.24	733	5	1.736	1.235	1.32
10	858	11	1.655	0.503	1.36	848	5	1.518	0.521	0.71	859	4		0.768	0.82
11	727	13	1.51	0.679	1.4	733	6	1.421	0.345	0.67	759	5	1.222	0.489	0.59
12	776	12	1.387	0.593	1.24	724	6	1.506	0.426	0.74	727	5	1.5	0.472	0.63
13	759	13	1.518	0.569	1.39	735	6	1.543	0.427	0.74	751	5	1.442	0.626	0.75
14	765	13	1.349	0.537	1.24	723	6	1.577	0.714	0.96	775	5	1.536	0.932	1.03
Mean			1.553	0.564	1.351			1.492	0.587	0.816			1.514	0.774	0.849

(number 12) in Figure 5.3. We note that $F(n)$ behavior strongly resembles the simulated data shown in Figure 5.2.

In order to show that similar scaling behavior is observed during relaxed normal breathing, in Figure 5.4 we compare DFA plots for three subjects during the spontaneous breathing session. Although RSA is not restricted to a narrow frequency band (as in paced breathing paradigms), it is evident that faster breathing frequencies produce a respiratory crossover at smaller scales. According to our prediction, slopes are always higher to the left of the crossover.

5.4 Discussion

In the original article introducing the DFA algorithm, Peng et al noted that the high α_{4-16} exponents obtained from healthy subjects are: "... probably due to the fact that on very short time scales, the physiologic interbeat interval fluctuation is dominated by the relatively smooth heartbeat oscillation associated with respiration ... (26). The only systematic study on the effects of breathing frequency on the DFA short-term exponent reported that a reduction in the respiration rate from 15 to 6 breaths per

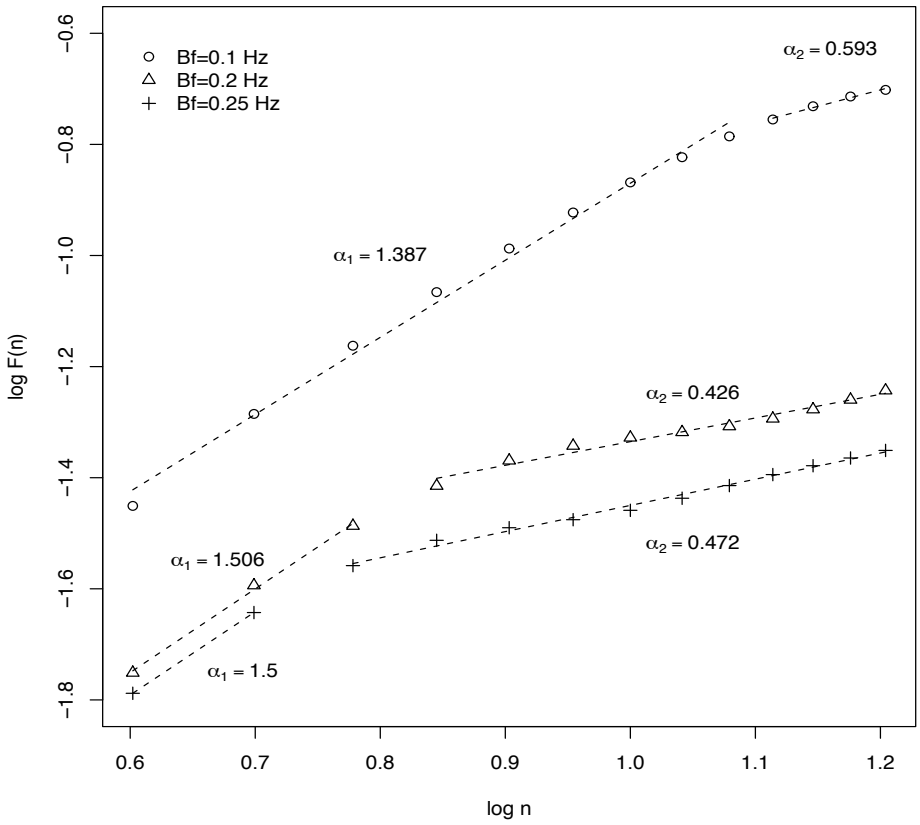

Figure 5.3: Crossover behavior of the F(n) function at different respiratory frequencies in one subject. Changes in scaling exponents indicate the location of the crossover. The crossover occurs at smaller scales as breathing becomes more rapid

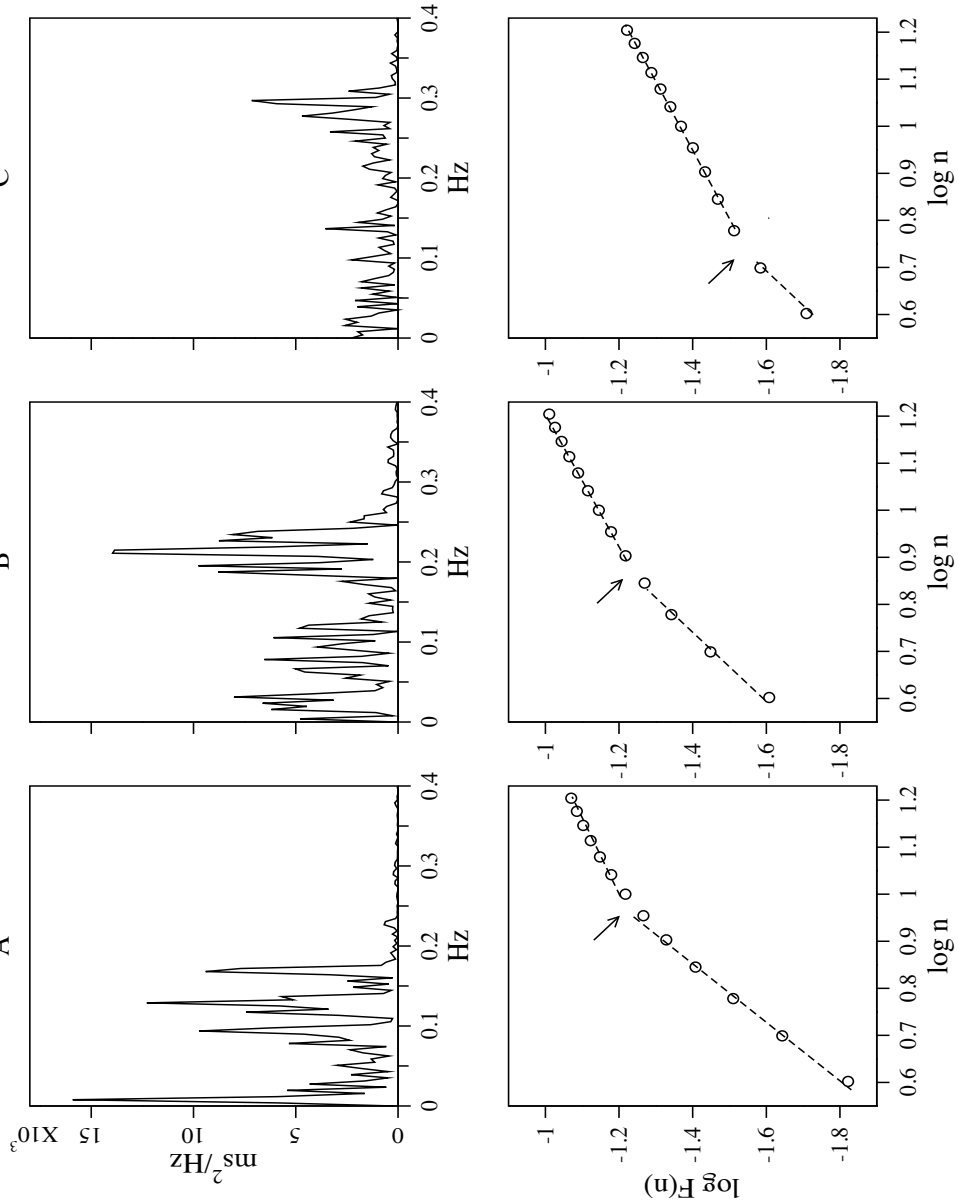

Figure 5.4: Crossover behavior of the F(n) function in three subjects (A, B and C) during spontaneous breathing. In the top row we observe a broad-band RSA at progressively faster frequencies as we move from subject A to subject C. Arrows on the DFA plots in the second row indicate scaling crossovers that are encountered at smaller scales for faster breathing frequencies

minute increased the scaling exponent from 0.83 ± 0.25 to 1.18 ± 0.27 (75). However, the authors offered no explanation for this effect.

Our study confirms the original suggestion by Peng et al (26) that the crossover at scales close to the respiratory period is caused by periodic breathing oscillations. As shown in section 1.3, this scaling behavior is similar in signals produced by the superposition of simulated correlated noise and sinusoidal trends. The superposition rule described by equation 5.3 explains the appearance of changes in scaling as a result of the competing contributions of the two signals at different time scales. Although, in the case of real IBI data we do not have independent signals, the principle of competing contributions can still be used to explain the scaling behavior of the $F(n)$ function. At short time scales (high frequencies), RSA is the dominant contribution in the IBI signal and $F(n)$ follows a constant local gradient with increasing n, leading to high scaling exponents. However, at scales longer than the respiratory crossover (given by equation 5.4), box sizes contain a complete respiratory cycle and RSA no longer contributes to the increases in $F(n)$ with increasing box size.

The results also explain the effects of breathing frequency alterations on estimations of the short-term DFA scaling exponent. In accordance with our second hypothesis, we showed that the changes in $F(n)$ scaling caused by changes in respiratory period, affected the scaling exponent α_{4-16}, which is usually considered to account for HRV short-term correlations. We found that α_{4-16} was significantly higher in the slow breathing condition when the α_1 exponent extended over a time scale range of 4 to approximately 12 beats, exerting a strong influence on the value of the α_{4-16} exponent. Conversely, the α_1 exponent extended over a shorter time scale range in the fast breathing condition and α_{4-16} was closer to α_2.

5.4.1 Re-interepreting results of previous studies

Our findings have important methodological implications for the interpretation of previous reports. The short-term DFA exponent has proven to be a more accurate predictor of mortality in patients with depressed left ventricular function after an acute myocardial infarction in comparison to the more common HRV measures (76). Thus, reduced α_{4-16} predicted both arrhythmic and nonarrhythmic cardiac death (77). Other studies showed that α_{4-16} was reduced in patients with dilated cardiomyopathy (78; 79), and

that reductions in the short-term DFA exponent are observed before the spontaneous onset of paroxysmal atrial fibrillation episodes (80).

In our study, however, we have shown that changes in breathing frequency produce significant alterations in the short-term DFA exponent that were related to effects of RSA behaving as a sinusoidal trend rather than to autonomic cardiac control. We also predicted and confirmed the exact direction of these alterations as a function of the breathing frequency and heart rate. In general, slow periodic breathing tends to increase the scaling exponent, while faster breathing significantly reduces it. Therefore, it is essential to consider both respiration and heart rate in order to correctly interpret short-term HRV scaling behavior. For example, faster and more irregular breathing (implying hyperventilation-related hypocapnia) may be responsible for the low scaling exponents observed in patients with cardiovascular diseases (81; 82; 83).

5.4.2 General conclusions and suggestions for further research

Our research calls for a reevaluation of fractal analysis of short-term HRV. As we have already noted, the use of scaling measures in physiological time series is interesting to the extent that it reveals information about the complex organization of underlining control mechanisms. Fractal long-term correlations in biological signals require the antagonistic interaction of nonlinearly coupled subsystems functioning and producing fluctuations at all scales (84). At high frequencies, however, HRV is dominated by RSA, a well studied mechanism attributable to respiratory modulation of vagal efferent outflow to the heart (85; 86). In addition, the time delays in sympathetic signal transduction caused by the intervention of second messenger cAMP for the depolarization of pacemaker cells in the sinoatrial node (72; 87), further support the notion that high-frequency HRV is driven by the parasympathetic system alone and is therefore not the right place to look for a substrate of complex nonlinear interactions.

This leads to the conclusion that DFA (and generally scaling analysis), is not valid when applied at small HRV scales. Alterations of the α_1 exponent by experimental manipulation or deviations from normal values in pathological populations cannot be attributed to a breakdown of fractal properties since those require a nonlinear coupling of multiple competing mechanisms functioning over a wide range of scales (88). We suggest that a more detailed examination of breathing parameters and vagal cardiac

influences would more adequately elucidate why the α_1 exponent is a good prognostic measure of various cardiovascular disorders.

Although we discourage the use of DFA for short-term HRV, we believe that it is a powerful algorithm to assess the correlation properties of cardiac IBI fluctuations at large scales. Ideally, long-term HRV scaling patterns are obtained by 24-hr ECG recordings. Evidence suggests, however, that shorter data segments of approximately 8200 samples (≈2-hr recordings) do not significantly reduce the reliability of the DFA algorithm (26; 63). This makes the use of DFA also suitable for behavioral experiments in laboratory settings.

The fractal 1/f noise observed in long-term HRV is also encountered in a certain class of physical systems which, for critical values of their parameters, exhibit complex organization characterized by long-term correlations among their individual components (89). In addition, Bak et al have shown that for some physical systems, organization at a critical state with fractal geometries, scale invariance and power law long-term correlations, happens spontaneously without the need for any external adjustment of parameters (90). Bak used the term Self-Organized Criticality (SOC) to describe this phenomenon which has been proposed as an explanation for fractal scale invariance in a wide variety of physical, biological and even social systems (91).

The characteristics of long-term correlations, scale invariance, and especially the absence of any fine tuning, make SOC an attractive principle to explain the dynamics of scale-free biological systems (1). The possibility of biological systems self-organizing in a critical state questions the traditional paradigm of homeostasis which postulates that in healthy organisms, physiologic control mechanisms operate to reduce variability generated by external perturbations in order to achieve an equilibrium-like state (92). SOC, on the contrary, suggests that the goal of physiologic control may be to maintain a complex variability over a broad range of scales rather than a steady or periodic state, even in resting conditions (93).

The advantages of SOC have been mostly investigated in computer models. It has been shown that the capacity of scale-free networks to generate fluctuations at all scales optimizes information transmission (94; 95), and information storage by maximizing the number of repeating complex activation patterns (96). Increased variability also allows a large number of different mappings between inputs and outputs which optimizes computational power without compromising the network's reliability (97). Finally,

fractal networks generate parallel trajectories in phase space, which means that despite increased variability, their dynamical evolution is still stable and controllable with minor corrective inputs (95; 96). Remarkably, all these seemingly contradictory information processing tasks are optimized simultaneously when a system operates near the critical point (58). Extrapolating the above results to cardiac dynamics, we can hypothesize that SOC in the cardiovascular system allows the heart to respond in a consistent manner to specific internal or external stimulation, while maintaining at the same time the flexibility to rapidly adjust to extreme perturbations.

The idea of complex variability is not new to psychophysiologists as the opposite extremes of strict periodicity (rigidity) and uncorrelated randomness are considered to contribute to inappropriate autonomic responses, characteristic of anxious and phobic patients (98; 99). In addition, there is a large amount of knowledge accumulated in the biopsychological literature regarding cardiac responsiveness to emotional and attentional stimuli. We believe that the application of new tools for the study of nonlinear dynamical systems may initiate a new line of psychophysiological research, where phasic cardiac responses to external stimuli can be used to test and support or reject the hypothesis of SOC in the cardiovascular system. In either case this will undoubtedly improve our understanding of how the various cardiac control mechanisms function as a whole in order to produce a fractal variability, and how this organization is disturbed in psychologically disordered states.

Chapter 6

The Effect of Parasympathetic Blockade on Fractal Analysis of Heart Rate Variability

6.1 Introduction

Cardiac vagal tone has been identified as a major risk factor for cardiovascular disease (100). Although efferent sympathetic traffic can be measured directly in conscious humans, parasympathetic outflow must be inferred from changes in the function of the effector organs (101). Thus, the variability in the heart rate signal (Heart Rate Variability; HRV) is one of the most common indirect indices of cardiac vagal tone (32). Decreased vagal function, implied by a reduced high-frequency HRV component, has been repeatedly observed in patients with cardiovascular disease and is considered a significant independent predictor of mortality in high-risk groups. For a detailed report on the relationship between HRV and cardiovascular disease, the interested reader can refer to the recent review by Thayer and Lane (100).

A relatively new area of research in cardiac physiology is the study of scaling characteristics and long-term correlations in heart rate fluctuations (54; 55; 102). The common notion has been that physiological systems, including the healthy heartbeat, are regulated according to the classical principal of homeostasis, operating to reduce variability and achieve an equilibrium-like state (92). However, under normal conditions, beat-to-beat heart rate fluctuations have been found to display the type of fractal-like

long-range correlations typically exhibited by dynamical systems near phase transition (26; 30; 62). The theory of Self-Organized Criticality (SOC) has been proposed to explain this type of spontaneous organization, which is observed in many physical and biological systems (57; 91). Interestingly, dynamical systems organized at a critical state demonstrate optimum information processing and transmission (94; 95). In addition, critical systems generate parallel trajectories in phase space and consequently, despite increased variability, their dynamical evolution remains stable and controllable with minor corrective inputs (95; 96). All of these advantages of systems functioning at a critical state are particularly significant for living organisms, which are constantly processing large amounts of information and are required to adapt rapidly to external perturbations while maintaining their internal consistency and function.

Various algorithms and methods have been proposed to assess the scaling characteristics of biological signals (103), but Detrended Fluctuation Analysis (DFA) remains the best-established algorithm to quantify correlation properties in nonstationary complex time series(63; 104). It has been applied in various research fields to study economics (46), climate temperature fluctuations (47), DNA (48), neural networks (49), and cardiac dynamics (26). The algorithm calculates a scaling exponent, *alpha* (α), which gives an estimate of the correlation properties of the time series.

The application of DFA to 24-hr interbeat interval (IBI) records of healthy individuals results in two frequency regions characterized by distinct scaling exponents. At scales extending from 16 to 3400 heartbeats (regime of long-term HRV), the value of the scaling exponent is approximately 1.0, indicating persistent, fractal long-term correlations reminiscent of critical dynamical systems. However, at higher frequencies of 4 to 16 heartbeats (regime of short-term HRV), the value of the α parameter is approximately 1.5, indicating stronger correlations (26). The scaling exponent relevant to short-term HRV is usually denoted as α_1 as opposed to α_2, which quantifies long-term HRV correlation behavior at lower frequencies.

Experimental applications of DFA to IBI data have largely focused on the short-term exponent, α_1. In their original article introducing the method, Peng et al found a reduced α_1 exponent (≈ 0.5) in patients with congestive heart failure (26). In a later study, reduced α_1 predicted both arrhythmic and non-arrhythmic cardiac death (77). Furthermore, it has been reported that α_1 is reduced in patients with dilated cardiomyopathy (78; 79) and also before the spontaneous onset of paroxysmal atrial

fibrillation episodes (80). In a recent study, low α_1 values proved to be a more accurate predictor of mortality in comparison to other HRV measures for patients with depressed left ventricular function after acute myocardial infarction (76).

Despite the use of the α_1 parameter as a prognostic measure, its physiological significance and specifically its relation to vagal tone, which is a major determinant of HRV at fast-frequencies (the regime of the α_1 exponent), remain poorly understood. The few studies that have examined the effect of pharmacological parasympathetic blockade on the α_1 exponent in healthy individuals reported elevated α_1 values, above 1.0, indicating strong correlations in the IBI signal after vagal abolishment (75; 105; 106). However, strong correlations at small time scales were also observed in healthy individuals with unimpaired autonomic control (26). Hence, it appears that healthy individuals and study participants under parasympathetic blockade both demonstrate similar short-term scaling characteristics.

In this study, we examined the effect of atropine on the short-term DFA exponent in nine healthy male subjects. Unlike previous studies, we attempt a coherent physiologic interpretation of our results based on the known effects of sinusoidal trends and mean heart rate on the DFA algorithm.

6.2 Methods

6.2.1 Participants

Nine healthy and physically fit male medicine students aged between 23 and 25 yrs participated in the study. None of the participants were on psychotropic medications, and no abnormalities were found in their history, physical examination, or baseline ECG.

6.2.2 Design

Six subjects were investigated twice: They received either atropine (0.03 mg/kg body weight i.v.) on day 1and metoprolol (up to 3X5 mg i.v.) on day 2 or the reverse order of drugs. Three subjects were investigated only once, receiving 3 X 5 ml of saline as a placebo condition. The latter individuals were informed that they received a drug influencing the regulatory characteristics of the cardiovascular system with no noticeable side effects. The study protocol was approved by the Ethical Committee of

the University of Bonn. A similar experimental design was previously used in various studies (8; 107; 108; 109).

6.2.3 Procedure

Participants were fitted with a peripheral intravenous line at 1 hr before the examination. In the laboratory, participants sat in a comfortable armchair in a semirecumbent position. After attaching and checking the electrodes and the measuring equipment, initial baseline HR was recorded for 10 min. Then, atropine was injected for 5 min or saline was injected for a maximum of 3 X 5 min. At 2 min after the injection, when physiological variables reach a steady state and possible measurement error is avoided (110), a second 10-min baseline recording was performed. HRV analysis was carried out for the last 5 min of each baseline period.

6.2.4 Data reduction and analysis

Heart rate was recorded from lead II of the ECG using a Gould amplifier. *KARDIA* Matlab software (74), designed for IBI data analysis, was used to obtain all HRV parameters and DFA scaling exponents. The HRV power spectrum was obtained after interpolating the IBI series with cubic splines at 2 Hz. The interpolated series was subsequently detrended by removing the best straight-line fit and multiplying by a Hanning window function. The discrete Fourier transform (DFT) was calculated by means of fast Fourier transform with 512 points. Finally, the Fourier power spectral density was obtained from the squared absolute value of the DFT, multiplied by the sampling period and divided by the number of samples in the signal.

KARDIA software implements the first-order DFA-1 algorithm as described elsewhere (26). In brief, the IBI series (of length N) is first integrated to calculate the sum of the differences between the ith interbeat interval $B(i)$ and the mean interbeat interval $\overline{B}$: $y(i) = \sum_{i=1}^{j}[B(i) - \overline{B}]$. Next, the integrated series $y(i)$ is divided into boxes of equal length n (measured in number of beats). Each box is subsequently detrended by subtracting a least-squares linear fit[1]

$$Y(i) = y(i) - y_{fit}(i) \tag{6.1}$$

[1]In the more general case of the DFA-m algorithm, detrending is performed by using order-m polynomial fits. In this paper, however, we used DFA-1, which fits a linear trend and is the most commonly used version of the algorithm

For a given box size n, we calculate the root mean square fluctuation

$$F(n) = \sqrt{\frac{1}{N}\sum_{i=1}^{N}[Y(i)]^2} \tag{6.2}$$

and this calculation is repeated over a range of box-sizes (time-scales) n to build up the relationship between fluctuations and time-scale (box size).

Normally, $F(n)$ will increase with time-scale n. A linear relationship on a log-log graph indicates the presence of scaling with an exponent quantified by the slope of the line (usually referred to as the α exponent). In this study, we calculated the short-term DFA exponent, α_1, for the region between 4 and 16 heartbeats in accordance with the original suggestion by Peng et al (26).

For uncorrelated time series (white noise), $F(n)$ is indicative of a random walk and the scaling exponent $\alpha = 0.5$. A scaling exponent larger than 0.5 indicates the presence of correlations in the original series (a large IBI is more likely to be followed by another large interval), while $0 < \alpha < 0.5$ indicates anti-correlations (large and small IBI values are more likely to alternate). Values of $\alpha > 1$ represent non-stationary behavior and specifically $\alpha = 1.5$ corresponds to highly correlated *Brown* noise. $\alpha = 1$ corresponds to $1/f$ pink noise, which can be interpreted as a balance between the complete step-by-step unpredictability of random signals and highly-correlated Brownian noise (50).

The effect of atropine on HRV measures was analyzed by means of an ANOVA with two repeated measures factors, before and after atropine.

6.3 Results

Table 6.1 shows the mean IBI, high-frequency HRV (HF), low-frequency HRV (LF), and α_1 scaling exponent values before and after atropine or placebo administration. Parasympathetic blockade caused a significant increase in the α_1 scaling exponent ($F_{(1,5)} = 19.55$, $p < 0.05$) and decreased the heart period ($F_{(1,5)} = 48$, $p < 0.05$) and HF power ($F_{(1,5)} = 7.29$, $p < 0.05$). The reduction in LF power after atropine was close to significant ($F_{(1,5)} = 6.212$, $p = 0.055$). Placebo did not produce any significant effects.

Figure 6.1 depicts the IBI records and power spectrum graphs for a single subject before and after atropine. Power spectra are calculated for the entire 5-min analysis,

Table 6.1: Interbeat intervals (IBI), high-frequency HRV (HF), low-frequency HRV (LF), and short-term HRV DFA scaling exponent (α_1) before and after administration of atropine or placebo. Standard deviations are given in parentheses.

		Pre-administration		Post-administration	
IBI	Atropine	938	(126)	562	(29)
	Placebo	959	(214)	959	(147)
HF	Atropine	362	(327)	0.7	(0.9)
	Placebo	475	(462)	342	(125)
LF	Atropine	531	(599)	3	(0.4)
	Placebo	253	(161)	397	(230)
α_1	Atropine	0.936	(0.17)	1.556	(0.202)
	Placebo	0.799	(0.243)	0.948	(0.173)

while the IBI series represent a shorter 50-sec data segment. The raw IBI data and the spectral analysis clearly depict two principal effects of atropine administration: a) an increase in heart rate, and b) elimination of fast parasympathetic-modulated oscillations at the respiratory frequency.

Firstly, the increase in heart rate is demonstrated by the number of heartbeats contained in a 50-sec segment: 54 heartbeats before atropine versus 89 heartbeats in the atropine condition. In this subject, atropine increased the heart rate from 67.7 to 109.8 bpm. Secondly, after atropine administration, the dominant respiratory oscillations just below 0.2Hz [Fig.6.1(C)] disappear completely, and the fastest frequency in the signal now has a lower value of 0.1Hz [Fig.6.1(D)].

To understand how the effect of atropine on fast respiratory oscillations influences the assessment of the DFA scaling exponent we need to look carefully at the properties of the DFA algorithm. For each box size n DFA calculates $F(n)$ fluctuations in the integrated and detrended IBI signal. Signals dominated by periodic oscillations with a period T were found to produce distinctive crossovers (changes of scaling) at a scale corresponding to period T (69). This occurs because $F(n)$ follows a constant local gradient for box sizes smaller than T ($n < T$) and increases steeply with increasing box size due to the absence of faster fluctuations in the signal. However, when $n > T$,

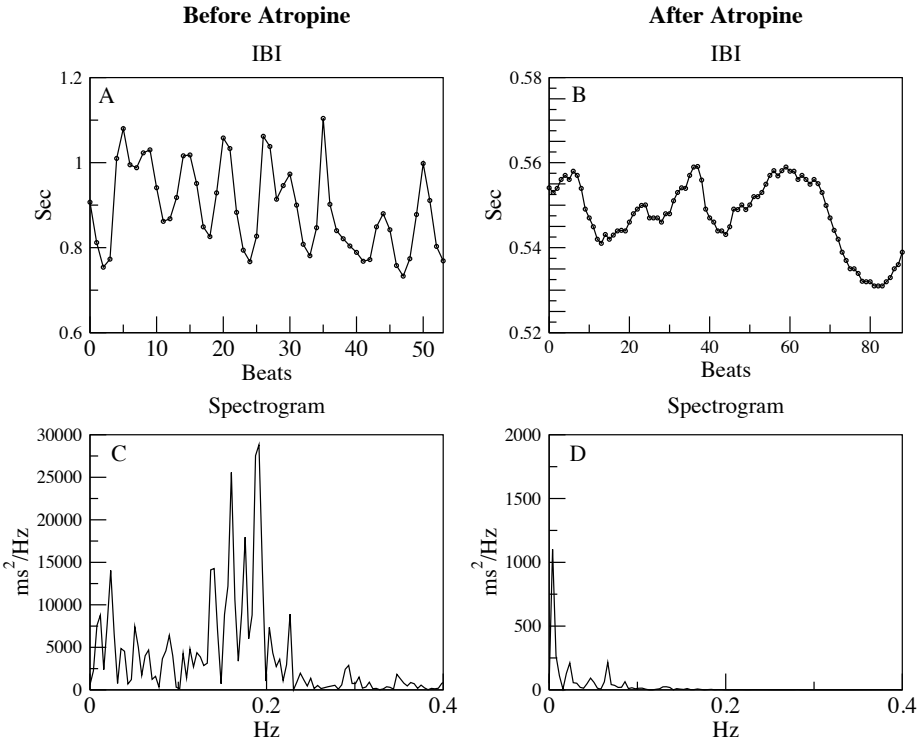

Figure 6.1: IBI series and power spectrum graphs for a single subject. IBI series illustrate a short 50-sec segment obtained from the entire 5-min record. The number of heartbeats in the two short segments indicates a heart rate increase in the atropine condition. The spectral graphs clearly show the elimination of fast respiratory oscillations just below 0.2 Hz after atropine administration. Note the difference in the scale of the figures before and after atropine

box sizes contain a complete period and repetitive oscillations no longer contribute to increases in $F(n)$ as box size becomes larger. This produces a characteristic plateau in the DFA plot of sinusoidal signals or signals dominated by strong periodic trends (69; 111).

Another way to conceptualize this effect is by analogy with a random walk, in which root mean square fluctuations at a specific time scale are visualized as the displacement of a random walker from his origin after taking a number of steps (equal to the number of samples in the examined time scale). Fast periodic oscillations force the walker to move continuously back and forth, ensuring that he remains at a short distance from his initial point. In this case, the displacement of the random walker does not depend on the number of steps or time scale (plateau region in the DFA plot). Slower non-periodic trends, on the contrary, allow the walker to drift further from his/her origin with the passage of time (high DFA slopes).

Figure 6.2 depicts the plot of log $F(n)$ against log n for the subject in Figure 1 before (circles) and after (squares) atropine. The mean heartbeat of this individual before atropine was 0.886 sec with RSA oscillations at around 0.2Hz, corresponding to a period of approximately 5 sec. Since the DFA algorithm measures time scales in number of heartbeats, the absolute time of each scale is determined by the average heartbeat interval. Thus, in order to find the scale that includes a whole respiratory cycle we divided the period of the cycle by the average heartbeat value, giving approximately $5/0.886 = 5.6$ heartbeats, which is the number of heartbeats containing a respiratory cycle. According to our previous analysis, DFA-assessed root mean square fluctuations increase when box size becomes larger for scales smaller than this respiratory scale ($n < T$), due to constant local gradients in the signal. Beyond the respiratory scale ($n > T$), however, the IBI signal is dominated by rapid periodic oscillations, therefore fluctuations do not tend to increase with increasing box size. We observe this effect in Figure 6.2, where an arrow indicates the location of the respiratory scale at $n = 6$ heartbeats. Before this critical scale, $F(n)$ increases steeply as n becomes bigger, yielding a scaling exponent $\alpha = 1.41$. For $7 < n < 16$ however, respiratory fluctuations dominate the IBI signal and $F(n)$ is less influenced by increasing scale (n) resulting in a significantly lower scaling exponent $\alpha = 0.54$.

After atropine administration, the fastest frequencies in the signal were at 0.1Hz, corresponding to a period of 10 sec. Given a mean heartbeat of 0.546 sec, the scale

that included a whole cycle was $10/0.546 \approx 18$ heartbeats. Thus, for windows $n < 18$, fluctuations $F(n)$ increased steeply with increasing scale, explaining the high scaling exponent $\alpha = 1.74$ for the entire $4 < n < 16$ region.

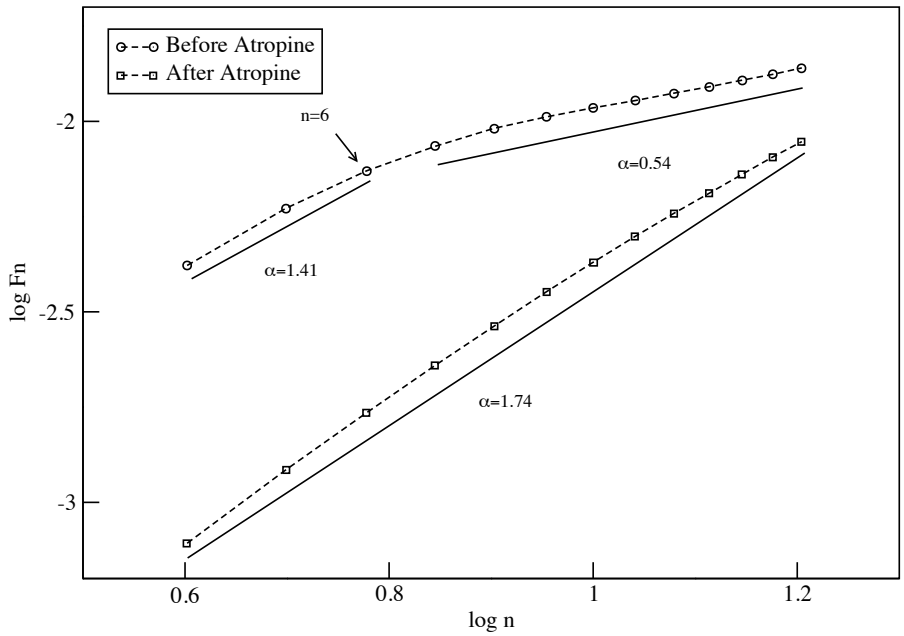

Figure 6.2: DFA plots for a single subject before and after atropine administration. Before atropine, respiratory oscillations produce a crossover that clearly divides the DFA plot into to two distinct scaling regions. For $n > 7$ fluctuations do not increase with increasing scale due to the periodicity in the signal. The resulting plateau region affects the estimation of the scaling exponent α_1 calculated for the entire region. Atropine eliminates fast respiratory oscillations and subsequently the plateau region in the DFA plot. This results in a higher α_1 exponent

6.4 Discussion

Our study addresses an important discrepancy in the literature on fractal properties of HRV. Fractal measures have been proposed as complementary to the more common time and frequency domain indices and, in many cases, have proven to be valid pre-

dictors of cardiovascular disease (76; 77; 78; 79; 80). In all previous studies, smaller short-term HRV scaling exponents in clinical populations have been attributed to a breakdown of fractal properties. Healthy individuals present larger short-term scaling exponents, which are considered to be indicative of a robust balance between different cardiac control mechanisms. The discrepancy arises from the confirmation by numerous authors that parasympathetic blockade also increases fractal indices of short-term HRV (75; 105; 106; 112; 113; 114; 115). It therefore appears that similar scaling properties characterize both individuals with healthy autonomic balance and those completely lacking parasympathetic cardiac control. On the contrary, given the importance of vagal tone for cardiovascular health, we would expect parasympathetic blockade to reduce fractal HRV indices as it does with other linear measures of short-term HRV.

We believe that the failure of previous authors to address this discordance stems from an incomplete understanding of the DFA algorithm and the way it is affected by systematic trends in the data. At least two studies have rigorously examined these effects using simulated signals (68; 69). Physiologists, however, have so far failed to apply this knowledge to the interpretation of results from real physiological data. Our present analysis explains how large scaling exponents in the atropine condition result from the elimination of parasympathetic respiratory-induced oscillations and the increase in heart rate. The combination of these two effects increases the range of scales in which cardiac dynamics are dominated by slow oscillations. Fluctuations in this range increase steeply as scales become larger, yielding high DFA exponents. A recent study demonstrated that high α_1 scaling exponents can also be produced by smooth period-like oscillations associated with RSA (111). In healthy subjects, RSA can be approximated by a sinusoidal trend whose period is given by the respiratory period. Perakakis et al have shown that slow breathing patterns, characteristic of healthy individuals, increase the range of scales dominated by smooth respiratory oscillations, resulting in higher α_1 exponents. Hence, two very different physiological conditions (high amplitude RSA at slow frequencies and parasympathetic blockade by pharmacological intervention) produce similar IBI correlation patterns at small time scales.

Another recent study showed how periodic IBI patterns associated with sleep apnea also produce alterations in DFA-assessed scaling exponents (116). As in the present case and in (111), these alterations do not necessarily reflect changes in autonomic cardiac control that could lead to a loss of fractal physiological complexity. Rather, all

three studies demonstrate that scaling parameters can be mere artifacts produced by the application of DFA to scales in which cardiac dynamics are dominated by smooth periodic trends associated either with respiration, sleep apnea, or even with the absence of fast fluctuations, as in the present case of parasympathetic blockade.

In another recent study, Tan et al. correctly observed that there is no consensus in the literature on what a "healthy" scaling exponent should be (117). This is not the case with more common HRV metrics closely associated with vagal tone, since high values are known to indicate a stronger parasympathetic influence on the heart. In contrast, fractal indices are not clearly associated with specific physiologic mechanisms and their relation to cardiovascular health is less understood. The use of fractal measures in cardiovascular physiology was initially triggered by the assumption that healthy cardiac dynamics resemble the dynamics of critical complex systems and therefore share their properties of maximum information processing and adaptability. This is only true for scaling exponents of around 1.0. Low exponents, closer to 0.5, indicate random fluctuations, while high values above 1.0 indicate strong correlations and reduced flexibility. As noted above, fractal HRV ($\alpha_1 \approx 1.0$) is observed in healthy individuals only at large scales (low frequencies). At small scales (fast frequencies), the heart rate signal is strongly correlated due to the presence of periodic oscillations associated with regular breathing.

Moreover, the very notion of applying fractal measures to a limited range of scales, in which signals are dominated by a single or a few control mechanisms, does not concur with the idea of investigating fractal correlations. It is well understood that fractal long-term correlations in biological signals require the antagonistic interaction between parasympathetic and sympathetic inputs together with a feedback of stochastic nature (84). In a limited scale-range, however, scaling parameters are more sensitive to trends associated with specific control mechanisms and cannot be attributed to an underlining holistic fractal organization in the cardiovascular system. We therefore assert that extreme caution is required in the interpretation of results on the scaling characteristics of short-term HRV. In this study, we showed why parasympathetic blockade results in large scaling exponents similar to those encountered in healthy individuals. This occurs independently of any possible underlying fractal organization of cardiac dynamics which could only be assessed for long-term HRV obtained from 24-hr recordings.

6.5 Conclusion

In this study, we have identified a serious methodological and mostly conceptual problem related to the application of fractal measures to short-term HRV. Although we strongly support that DFA is not valid when applied at small scales, we still encourage research on the fractal properties of long-term cardiac dynamics. If further research confirms the hypothesis that the cardiovascular system is organized in a critical state, this would open up the way to a new understanding of physiologic control and could improve the diagnosis of disordered cardiac dynamics.

Chapter 7

Discussion

In this doctoral dissertation we explored in depth the conceptual and methodological problems related to the application of fractal measures to short-term heart rate variability. Fractal analysis of HRV is a relatively new field of research in cardiovascular physiology and a completely uncharted territory for psychophysiologists. Most of the algorithms used for the assessment of fractal properties in biological signals were elaborated by theoretical physicists in the early nineties and are continuously being refined and improved both by physicists and engineers. Physiologists, and generally researchers without a solid mathematical background, have started to include this new type of analysis in their experiments and to report quantitative results that in many cases show fractal measures to be valid predictors of cardiovascular health. The physiological interpretation of these results, however, is usually extremely limited and is based on theories developed by physicists investigating complex systems of inanimate matter.

Collaboration between scientists is always positive, but particularly in this novel area of research, it is fundamental. The articles presented in this dissertation were the product of such collaboration between theoretical physicists and psychophysiologists. They represent an attempt to explore the subject of fractal analysis of HRV, keeping always in mind the physiological characteristics of the cardiovascular system, but without simplifying the mathematical formality.

The interest in fractal analysis of HRV was triggered by the conceptual novelty that this new type of analysis brings to physiological research. Homeostasis is one of the oldest concepts in physiology. According to the homeostatic theory, physiologic control

mechanisms operate to reduce variability produced by external inputs to the organism. The goal is to maintain a steady state that ensures the proper function of the entire organism. In this context, erratic fluctuations observed in physiological signals are considered as "noise" deriving from ongoing external stimulation. This noise is regarded as irrelevant to the internal characteristics of the system and thus it does not provide any useful information for researchers. These ideas are not only discussed on a theoretical level, but also determine the methodologies used in physiological research. Averaging signals over many trials and subjects in order to increase the "signal to noise" ratio is an interesting example of how the theory of homeostasis pertains to experimental research. Averaging signals is a prominent experimental paradigm both in cardiovascular and brain research, where event-related potentials (ERPs) have monopolized the interest of psychophysiologists for many decades.

The homeostatic theory is not the only reason why irregular fluctuations in biological signals are commonly regarded as uninteresting noise. The other reason is the tendency to perceive physiological systems (and systems in general) as simple and linear. The linearity in our every day thinking, where causes are directly related to specific effects, permeates the way we view biological systems as well. When observing fluctuations in a physiological variable, for example, it is natural to think that a sudden increase in amplitude is directly associated to a specific event in the internal or external environment of the organism. Moreover, large increases are naturally associated with large scale events.

Although homeostatic control and linear interactions are undoubtedly important for the understanding of physiological function, a new vision of how natural systems work is beginning to surface in science. Starting from physics and expanding to other areas, the remarkable complexity of nature is beginning to be acknowledged and investigated. While we tend to think of the experimental physicist as a scientist who tries to isolate nature in a laboratory in order to control all irrelevant variables and create simple linear interactions in the system of interest, we should also start to recognize the physicist who lets nature behave freely in all its magnificent complexity, while he or she observes general statistical characteristics and discovers remarkable commonalities between seemingly unrelated systems.

Complexity is a new science, or a new way of making science that is complementary to reductionism. Reductionistic approaches have long defined our understanding

about how nature works. Complexity scientists view systems as wholes interacting in nonlinear and complex manners with their individual parts and their environments. Applied to physiology, this new approach is not treating signals as meaningful events superimposed on background random noise. What was previously perceived as random and trivial is now thought to contain valuable information about the functional organization of the system. Irregular fluctuations reflect an intrinsic variability arising from the complex interactions between the system's subparts. If properly quantified, these fluctuations may reveal information at least as important as the information derived from the examination of the system's response to external stimuli.

Complexity scientists analyzing the statistical characteristics of fluctuating time series were surprised to discover unexplainable similarities between different systems. Perhaps the most distinguished property shared by many systems is self-similarity, or scale invariance. When scale-invariant, fractal correlations were first observed in the heart rate signal, researchers started to hypothesize on the advantages of such organization: increased adaptability to external and internal stimuli and yet resistance to random perturbations that could drive and lock the system to one or a few specific frequencies, eliminating its flexibility to an unstable environment. However, a deviation from this fractal temporal organization was observed at small scales. While fractal correlations spanned the range from ultra-low to low-frequencies, fast-frequencies were dominated by strong correlations that were associated with breathing-related smooth oscillations.

At that point it would have been reasonable to assume that fractal correlations, indicative of adaptive scale invariance in the cardiovascular system, are dominant at low frequencies, while fluctuations at fast frequencies are mainly determined by the parasympathetic-mediated respiratory sinus arrhythmia that produces a synchrony between respiration and heart rate. Curiously, instead of making this clear distinction between low and fast frequencies, researchers continued to investigate the "fractal" properties of heart rate variability at fast frequencies. Even worse, due to the fact that less recording time is required to obtain valid estimates of short-term scaling exponents, the vast majority of studies on fractal analysis of HRV have been so far concerned with the fast frequencies regime.

A theoretical analysis of the concept of fractals in fluctuating time series, like the one we attempted so far in this discussion, is sufficient to invalidate the use of fractal

measures in short-term HRV. In this dissertation, however, we went one step further and conducted two experimental studies to clearly demonstrate the above point. In the first study, we showed the exact relationship between respiration and scaling exponents of short-term HRV. We proved that respiratory driven oscillations produce a clear crossover on HRV scaling. This crossover depends on breathing frequency and mean heart period and is independent of any possible underlining fractal organization in the cardiovascular system. We also showed how the exact location of the respiratory crossover affects the estimate of the short-term HRV scaling exponent. Slow breathing tends to increase the α_1 exponent, while faster breathing produces the opposite effect. This again is independent of the intrinsic dynamics of the cardiovascular system and solely depends on respiration rate. The results presented in this study were not only statistically significant, but more important, they were consistent with a mathematical explanation of how scaling analysis is influenced by periodic trends in the data.

In the second study, we used the same mathematical logic to interpret the effects of parasympathetic blockade on fractal analysis of HRV. Again, we showed that the increased correlations after vagal blockade that were observed in many previous studies, are not related to any intrinsic properties of cardiac dynamics, but are a mere artifact of local trends present in the data.

The inevitable conclusion after the theoretical and experimental analysis presented in this dissertation is that fractal analysis of short-term HRV is both conceptually and technically wrong. Conceptually, because at short time scales HRV is dominated by breathing-related periodic oscillations, whereas fractal variability requires a complex interaction between two or more control mechanisms, allowing a delicate balance at a critical state and producing fluctuations at all scales (scale invariance). Technically, because at short scales fractal measures are sensitive to systematic periodic and other trends in the data.

There is, however, strong evidence of fractal correlations dominating long-term HRV. New studies need to be designed to explore the advantages provided by this type of temporal organization of cardiac dynamics and scientists from different fields need to collaborate towards this goal. Psychophysiologists can actively participate in this endeavor. Their firm background in cardiovascular physiology and extensive research on cardiac responsiveness under different emotional and attentional states can significantly enrich the quest for a better understanding of how and why autonomic control

produces long-term correlations and scale invariance in cardiac dynamics. Such understanding may also indicate new ways to diagnose perturbed autonomic organization in psychologically and/or physiologically disordered states.

Bibliography

[1] T. Gisiger. **Scale invariance in biology: coincidence or footprint of a universal mechanism?** *Biological Reviews*, **76**(02):161–209, 2001. xv, 8, 12, 13, 14, 16, 17, 47

[2] A.L. Goldberger, L.A.N. Amaral, J.M. Hausdorff, P.C. Ivanov, C.K. Peng, and H.E. Stanley. **Fractal dynamics in physiology: alterations with disease and aging**. *Proceedings of the National Academy of Sciences*, **99**(90001):2466–2472, 2002. xv, 8, 17, 18, 73

[3] R.E. Kleiger, P.K. Stein, and J.T. Bigger. **Heart rate variability: measurement and clinical utility**. *Annals of Noninvasive Electrocardiology*, **10**(1):88–101, 2005. 5, 7, 8, 9, 38

[4] J.T. Bigger Jr, R.E. Kleiger, J.L. Fleiss, L.M. Rolnitzky, R.C. Steinman, and J.P. Miller. **Components of heart rate variability measured during healing of acute myocardial infarction.** *The American journal of cardiology*, **61**(4):208, 1988. 6

[5] T. Ritz, B. Dahme, and W.T. Roth. **Behavioral interventions in asthma biofeedback techniques**. *Journal of psychosomatic research*, **56**(6):711–720, 2004. 6

[6] G.G. Berntson, D.L. Lozano, and Y.J. Chen. **Filter properties of root mean square successive difference (RMSSD) for heart rate**. *Psychophysiology*, **42**(2):246–252, 2005. 6

[7] J. Penttila, A. Helminen, T. Jartti, T. Kuusela, H.V. Huikuri, M.P. Tulppo, R. Coffeng, and H. Scheinin. **Time domain, geometrical and frequency domain analysis of cardiac vagal outflow: effects of various respiratory patterns**. *Clinical Physiology*, **21**(3):365–376, 2001. 6

[8] S. Akselrod, D. Gordon, F.A. Ubel, D.C. Shannon, A.C. Berger, and R.J. Cohen. **Power spectrum analysis of heart rate fluctuation: a quantitative probe of beat-to-beat cardiovascular control**. *Science*, **213**(4504):220–222, 1981. 6, 52

[9] D.M. Bloomfield, A. Magnano, J.T. Bigger, H. Rivadeneira, M. Parides, and R.C. Steinman. **Comparison of spontaneous vs. metronome-guided breathing on assessment of vagal modulation using RR variability**. *American Journal of Physiology- Heart and Circulatory Physiology*, **280**(3):1145–1150, 2001. 7

[10] M.L. Appel, R.D. Berger, J.P. Saul, J.M. Smith, and R.J. Cohen. **Beat to beat variability in cardiovascular variables: Noise or music?** *Journal of the American College of Cardiology*, **14**(5):1139–1148, 1989. 7

[11] R. Furlan, S. Guzzetti, W. Crivellaro, S. Dassi, M. Tinelli, G. Baselli, S. Cerutti, F. Lombardi, M. Pagani, and A. Malliani. **Continuous 24-hour assessment of the neural regulation of systemic arterial pressure and RR variabilities in ambulant subjects**. *Circulation*, **81**(2):537–547, 1990. 7

[12] G.E. Billman and J.P. Dujardin. **Dynamic changes in cardiac vagal tone as measured by time-series analysis**. *American Journal of Physiology- Heart and Circulatory Physiology*, **258**(3):896–902, 1990. 7

[13] O. Odemuyiwa, M. Malik, T. Farrell, Y. Bashir, J. Poloniecki, and J. Camm. **Comparison of the predictive characteristics of heart rate variability index and left ventricular ejection fraction for all-cause mortality, arrhythmic events and sudden death after acute myocardial infarction.** *The American journal of cardiology*, **68**(5):434, 1991. 7

[14] D.M. Bloomfield, E.S. Kaufman, and J.T. Bigger. **Passive head-up tilt and actively standing up produce similar overall autonomic balance**. *Am Heart J*, **134**:136, 1997. 7

[15] J.A. Taylor, D.L. Carr, C.W. Myers, and D.L. Eckberg. **Mechanisms underlying very-low-frequency RR-interval oscillations in humans**. *Circulation*, **98**(6):547–555, 1998. 7

[16] R.I. Kitney. **An analysis of the thermoregulatory influences on heart-rate variability**. *The Study of Heart Rate Variability*, pages 81–106, 1980. 7

[17] J.T. Bigger, J.L. Fleiss, R.C. Steinman, L.M. Rolnitzky, R.E. Kleiger, and J.N. Rottman. **Frequency domain measures of heart period variability and mortality after myocardial infarction**. *Circulation*, **85**(1):164–171, 1992. 7

[18] M. Barahona and C.S. Poon. **Detection of Nonlinear Dynamics in Short, Noisy Time-Series**. *Nature*, **381**(6579):215–217, 1996. 8

[19] G. Sugihara, W. Allan, D. Sobel, and K.D. Allan. **Nonlinear control of heart rate variability in human infants**. *Proceedings of the National Academy of Sciences*, **93**(6):2608–2613, 1996. 8

[20] P.C. Ivanov, M.G. Rosenblum, C.K. Peng, J. Mietus, S. Havlin, H.E. Stanley, and A.L. Goldberger. **Scaling behaviour of heartbeat intervals obtained by wavelet-based time-series analysis.** *Nature*, **383**(6598):323, 1996. 8

[21] D. Hoyer, K. Schmidt, R. Bauer, U. Zwiener, M. Kohler, B. Luthke, and M. Eiselt. **Nonlinear analysis of heart rate and respiratory dynamics**. *IEEE engineering in medicine and biology magazine*, **16**(1):31–39, 1997. 8

[22] Y. Ashkenazy, P.C. Ivanov, S. Havlin, C.K. Peng, A.L. Goldberger, and H.E. Stanley. **Magnitude and sign correlations in heartbeat fluctuations**. *Physical Review Letters*, **86**(9):1900–1903, 2001. 8

[23] B.B. Mandelbrot. *The fractal geometry of nature*. WH Freeman, New York, 1983. 8, 11, 33

BIBLIOGRAPHY

[24] J.T. Bigger, R.C. Steinman, L.M. Rolnitzky, J.L. Fleiss, P. Albrecht, and R.J. Cohen. **Power law behavior of RR-interval variability in healthy middle-aged persons, patients with recent acute myocardial infarction, and patients with heart transplants**. *Circulation*, **93**(12):2142–2151, 1996. 8

[25] A. Schumacher. **Linear and nonlinear approaches to the analysis of RR interval variability**. *Biological Research for Nursing*, **5**(3):211, 2004. 8

[26] C.K. Peng, S. Havlin, H.E. Stanley, and A.L. Goldberger. **Quantification of scaling exponents and crossover phenomena in nonstationary heartbeat time series**. *Chaos: An Interdisciplinary Journal of Nonlinear Science*, **5**:82, 1995. 11, 17, 19, 23, 26, 35, 36, 41, 42, 45, 47, 50, 51, 52, 53, 73, 74

[27] J.E. McNamee. **Fractal perspectives in pulmonary physiology**. *Journal of Applied Physiology*, **71**(1):1, 1991. 12

[28] D. Paumgartner, G. Losa, and E.R. Weibel. **Resolution effect on the stereological estimation of surface and volume and its interpretation in terms of fractal dimensions.** *Journal of microscopy*, **121**(Pt 1):51, 1981. 12

[29] W.H. Press. **Flicker noises in astronomy and elsewhere**. *Comments on Modern Physics*, **7**(4):103–119, 1978. 17

[30] M. Kobayashi and T. Musha. **1/f fluctuation of heartbeat period**. *IEEE Transactions on Biomedical Engineering*, **29**(6):456–457, June 1982. 17, 18, 34, 50

[31] P. Mansier, J. Clairambault, N. Charlotte, C. Médigue, C. Vermeiren, G. LePape, F. Carré, A. Gounaropoulou, and B. Swynghedauw. **Linear and non-linear analyses of heart rate variability: a minireview**. *Cardiovascular Research*, **31**(3):371, 1996. 21

[32] A.J. Camm, M. Malik, J.T. Bigger Jr, et al. **Heart rate variability: standards of measurement, physiological interpretation and clinical use. Task force of the European Society of Cardiology and the North American Society of Pacing and Electrophysiology**. *Circulation*, **93**:1043–1065, 1996. 21, 34, 49

[33] J.L.A. Carvalho, A.F. da Rocha, F.A.O. Nascimento, J. Souza Neto, and L.F. Junqueira Jr. **Development of a Matlab software for analysis of heart rate variability**. In B. Yuan and X. Tang, editors, *6th International Conference on Signal Processing*, **2**, pages 1488–1492, Beijing, China, 2002. Institute of Electrical and Electronics Engineers, Inc. 21, 29, 40

[34] R. Maestri and G.D. Pinna. **POLYAN: a computer program for polyparametric analysis of cardiorespiratory variability signals**. *Computer Methods and Programs in Biomedicine*, **56**(1):37–48, 1998. 21

[35] J.P. Niskanen, M.P. Tarvainen, P.O. Ranta-aho, and P.A. Karjalainen. **Software for advanced HRV analysis**. *Computer Methods and Programs in Biomedicine*, **76**(1):73–81, 2004. 22

[36] P. Perakakis, M. Joffily, and M. Taylor. **KARDIA project**. `https://sourceforge.net/projects/mykardia/`, accessed June 29, 2009. 22

[37] J.R. Jennings, W.K. Bberg, J.S. Hutcheson, P. Obrist, S. Porges, and G. Turpin. **Publication guidelines for heart rate studies in man**. *Psychophysiology*, **18**(3):226–231, 1981. 22

[38] M.M. Bradley, M. Codispoti, B.N. Cuthbert, and P.J. Lang. **Emotion and motivation I: defensive and appetitive reactions in picture processing**. *Emotion*, **1**(3):276–298, 2001. 22

[39] A. Ohman, A. Hamm, and K. Hugdahl. **Cognition and the autonomic nervous system: orienting, anticipation, and conditioning**. *Handbook of Psychophysiology*, pages 533–575, 2000. 22

[40] T.P. Dinh, H. Perrault, P. Calabrese, A. Eberhard, and G. Benchetrit. **New statistical method for detection and quantification of respiratory sinus arrhythmia**. *IEEE Transactions on Biomedical Engineering*, **46**(9):1161–1165, 1999. 24, 75

[41] G.A. Reyes del Paso and J. Vila. **The continuing problem of incorrect heart rate estimation in psychophysiological studies: an off-line solution for cardiotachometer users**. *Biological Psychology*, **48**(3):269–279, 1998. 24

[42] F.K. Graham. **Constraints on measuring heart rate and period sequentially through real and cardiac time**. *Psychophysiology*, **15**(5):492–495, 1978. 25, 75

[43] J. Vila, P. Guerra, M.Á. Muñoz, C. Vico, M.I. Viedma-del Jesús, L.C. Delgado, P. Perakakis, E. Kley, J.L. Mata, and S. Rodríguez. **Cardiac defense: from attention to action**. *International Journal of Psychophysiology*, **66**(3):169–182, 2007. 25, 75

[44] H. Jokinen, J. Ollila, and O. Aumala. **On windowing effects in estimating averaged periodograms of noisy signals**. *Measurement*, **28**(3):197–207, 2000. 26

[45] P. Stoica and R.L. Moses. *Introduction to Spectral Analysis*. Prentice Hall Upper Saddle River, NJ, 1997. 26

[46] R. Weron. **Estimating long-range dependence: Finite sample properties and confidence intervals**. *Physica A*, **312**(1-2):285–299, 2002. 26, 35, 50

[47] D. Vjushin, R.B. Govindan, S. Brenner, A. Bunde, S. Havlin, and H.J. Schellnhuber. **Lack of scaling in global climate models**. *Journal of Physics Condensed Matter*, **14**(9):2275–2282, 2002. 26, 35, 50

[48] S.V. Buldyrev, N.V. Dokholyan, A.L. Goldberger, S. Havlin, C.K. Peng, H.E. Stanley, and G.M. Viswanathan. **Analysis of DNA sequences using methods of statistical physics**. *Physica A*, **249**(1):430–438, 1998. 26, 35, 50

[49] C.J. Stam, T. Montez, B.F. Jones, S. Rombouts, Y. van der Made, Y.A.L. Pijnenburg, and P. Scheltens. **Disturbed fluctuations of resting state EEG synchronization in Alzheimer's disease**. *Clinical Neurophysiology*, **116**(3):708–715, 2005. 26, 35, 50

[50] C.K. Peng, S.V. Buldyrev, A.L. Goldberger, S. Havlin, F. Sciortino, M. Simons, and H.E. Stanley. **Long-range correlations in nucleotide sequences**. *Nature*, **356**:168–170, 1992. 27, 35, 53

[51] Free Software Foundation. **GNU General Public License**, 2007. 29

[52] P.J. Lang, M.M. Bradley, and B.N. Cuthbert. **International affective picture system (IAPS): technical manual and affective ratings**. *Gainesville, FL: The Center for Research in Psychophysiology, University of Florida*, 1995. 29

[53] P.J. Lang, R.F. Simons, and M.T. Balaban. *Attention and Orienting: Sensory and Motivational Processes*. Lawrence Erlbaum Associates, 1997. 30

[54] H.E. Stanley, L.A.N. Amaral, S.V. Buldyrev, A.L. Goldberger, S. Havlin, H. Leschhorn, P. Maass, H.A. Makse, C.K. Peng, M.A. Salinger, et al. **Scaling and universality in animate and inanimate systems**. *Physica A*, **231**:20–48, 1996. 33, 49

[55] H.E. Stanley, L.A.N. Amaral, P. Gopikrishnan, P.C. Ivanov, T.H. Keitt, and V. Plerou. **Scale invariance and universality: Organizing principles in complex systems**. *Physica A*, **281**(1-4):60–68, 2000. 33, 34, 49, 73

[56] P.C. Ivanov, L.A.N. Amaral, A.L. Goldberger, S. Havlin, M.G. Rosenblum, Z.R. Struzik, and H.E. Stanley. **Multifractality in human heartbeat dynamics**. *Nature*, **399**:461–465, 1999. 33

[57] P. Bak, C. Tang, and K. Wiesenfeld. **Self-organized criticality: An explanation of the 1/f noise**. *Physical Review Letters*, **59**(4):381–384, 1987. 34, 50

[58] J.M. Beggs. **The criticality hypothesis: How local cortical networks might optimize information processing**. *Philosophical Transactions of the Royal Society A*, **366**(1864):329–343, 2008. 34, 48

[59] H.J. Jensen. *Self-organized criticality: Emergent complex behavior in physical and biological systems*. Cambridge University Press, London, 1998. 34

[60] G.G. Berntson, J. Thomas Bigger, D.L. Eckberg, P. Grossman, P.G. Kaufmann, M. Malik, H.N. Nagaraja, S.W. Porges, J.P. Saul, P.H. Stone, et al. **Heart rate variability: Origins, methods, and interpretive caveats**. *Psychophysiology*, **34**(6):623–648, 1997. 34

[61] J.J.B. Allen, A.S. Chambers, and D.N. Towers. **The many metrics of cardiac chronotropy: A pragmatic primer and a brief comparison of metrics**. *Biological Psychology*, **74**(2):243–262, 2007. 34

[62] J.P. Saul, P. Albrecht, R.D. Berger, and R.J. Cohen. **Analysis of long term heart rate variability: Methods, 1/f scaling and implications.** *Computers in Cardiology*, **14**:419–22, 1988. 34, 50

[63] A. Eke, P. Herman, L. Kocsis, and LR Kozak. **Fractal characterization of complexity in temporal physiological signals**. *Physiological Measurement*, **23**(1):1–38, 2002. 34, 47, 50

[64] H.V. Huikuri, T.H. Mäkikallio, and J. Perkiömäki. **Measurement of heart rate variability by methods based on nonlinear dynamics**. *Journal of Electrocardiology*, **36**:95–99, 2003. 34

[65] C.K. Peng, J. Mietus, J.M. Hausdorff, S. Havlin, H.E. Stanley, and A.L. Goldberger. **Long-range anticorrelations and non-Gaussian behavior of the heartbeat**. *Physical Review Letters*, **70**(9):1343–1346, 1993. 34

[66] A.L. Goldberger, C.K. Peng, and L.A. Lipsitz. **What is physiologic complexity and how does it change with aging and disease?** *Neurobiology of Aging*, **23**:23–26, 2002. 34, 73

[67] A.L. Goldberger, L.A.N. Amaral, L. Glass, J.M. Hausdorff, P.Ch. Ivanov, R.G. Mark, J.E. Mietus, G.B. Moody, C.K. Peng, and H.E. Stanley. **PhysioBank, PhysioToolkit, and PhysioNet: Components of a new research resource for complex physiologic signals**. *Circulation*, **101**(23):215–220, 2000. 36

[68] J.W. Kantelhardt, E. Koscielny-Bunde, H.H.A. Rego, S. Havlin, and A. Bunde. **Detecting long-range correlations with detrended fluctuation analysis**. *Physica A*, **295**(3-4):441–454, 2001. 36, 58, 74

[69] K. Hu, P.C. Ivanov, Z. Chen, P. Carpena, and H.E. Stanley. **Effect of trends on detrended fluctuation analysis**. *Physical Review E*, **64**(1):011114–011119, 2001. 36, 38, 54, 56, 58, 74

[70] Z. Chen, K. Hu, P. Carpena, P. Bernaola-Galvan, H.E. Stanley, and P.C. Ivanov. **Effect of nonlinear filters on detrended fluctuation analysis**. *Physical Review E*, **71**(1):11104, 2005. 36

[71] Z. Chen, P.C. Ivanov, K. Hu, and H.E. Stanley. **Effect of nonstationarities on detrended fluctuation analysis**. *Physical Review E*, **65**(4):41107, 2002. 36

[72] G.G. Berntson, J.T. Cacioppo, and K.S. Quigley. **Respiratory sinus arrhythmia: Autonomic origins, physiological mechanisms, and psychophysiological implications**. *Psychophysiology*, **30**(2):183–196, 1993. 38, 46, 74

[73] F.A. Boiten, N.H. Frijda, and C.J. Wientjes. **Emotions and respiratory patterns: Review and critical analysis**. *International Journal of Psychophysiology*, **17**(2):103–128, 1994. 38

[74] P. Perakakis, P. Guerra, J.L. Mata-Martin, L. Anllo-Vento, and J. Vila. **KARDIA: An open source graphic user interface for the analysis of cardiac interbeat intervals**. *Psychophysiology*, **45**(s1):addendum, 2008. 40, 52, 75

[75] J. Penttila, A. Helminen, T. Jartti, T. Kuusela, H.V. Huikuri, M.P. Tulppo, and H. Scheinin. **Effect of cardiac vagal outflow on complexity and fractal correlation properties of heart rate dynamics.** *Autonomic & Autacoid Pharmacology*, **23**(3):173, 2003. 45, 51, 58

[76] P.K. Stein, J.I. Barzilay, P.H. Chaves, S.Q. Mistretta, P.P. Domitrovich, J.S. Gottdiener, M.W. Rich, and R.E. Kleiger. **Novel measures of heart rate variability predict cardiovascular mortality in older**

BIBLIOGRAPHY

adults independent of traditional cardiovascular risk factors: The cardiovascular health study (CHS). *Journal of Cardiovascular Electrophysiology*, **19**(11):1169–1174, 2008. 45, 51, 58

[77] H.V. Huikuri, T.H. Mäkikallio, C.K. Peng, A.L. Goldberger, U. Hintze, and M. Moller. **Fractal correlation properties of RR interval dynamics and mortality in patients with depressed left ventricular function after an acute myocardial infarction**. *Circulation*, **101**(1):47–53, 2000. 45, 50, 58

[78] N.G. Mahon, A.E. Hedman, M. Padula, Y. Gang, I. Savelieva, J.E.P. Waktare, M.M. Malik, H.V. Huikuri, and W.J. McKenna. **Fractal correlation properties of RR interval dynamics in asymptomatic relatives of patients with dilated cardiomyopathy**. *European Journal of Heart Failure*, **4**(2):151–158, 2002. 45, 50, 58

[79] A. Voss, R. Schroeder, S. Truebner, M. Goernig, H.R. Figulla, and A. Schirdewan. **Comparison of nonlinear methods symbolic dynamics, detrended fluctuation, and Poincaré plot analysis in risk stratification in patients with dilated cardiomyopathy**. *Chaos: An Interdisciplinary Journal of Nonlinear Science*, **17**:015120, 2007. 45, 50, 58

[80] S. Vikman, T.H. Makikallio, S. Yli-Mayry, S. Pikkujamsa, A.M. Koivisto, P. Reinikainen, K.E.J. Airaksinen, and H.V. Huikuri. **Altered complexity and correlation properties of RR interval dynamics before the spontaneous onset of paroxysmal atrial fibrillation**. *Circulation*, **100**(20):2079–2084, 1999. 46, 51, 58

[81] I. Dimopoulou, O.K. Tsintzas, P.A. Alivizatos, and G.E. Tzelepis. **Pattern of breathing during progressive exercise in chronic heart failure**. *International Journal of Cardiology*, **81**(2-3):117–121, 2001. 46

[82] B.D. Johnson, K.C. Beck, L.J. Olson, K.A. O'Malley, T.G. Allison, R.W. Squires, and G.T. Gau. **Ventilatory constraints during exercise in patients with chronic heart failure**. *Chest*, **117**(2):321–332, 2000. 46

[83] J.T. Mazzara, S.M. Ayres, and W.J. Grace. **Extreme hypocapnia in the critically ill patient**. *American Journal of Medicine*, **56**(4):450–6, 1974. 46

[84] P.C. Ivanov, LA Nunes Amaral, AL Goldberger, and HE Stanley. **Stochastic feedback and the regulation of biological rhythms**. *Europhysics Letters*, **43**(4):363–368, 1998. 46, 59, 76

[85] J.W. Denver, S.F. Reed, and S.W. Porges. **Methodological issues in the quantification of respiratory sinus arrhythmia**. *Biological Psychology*, **74**(2):286–294, 2007. 46

[86] P. Grossman and E.W. Taylor. **Toward understanding respiratory sinus arrhythmia: Relations to cardiac vagal tone, evolution and biobehavioral functions**. *Biological Psychology*, **74**(2):263–285, 2007. 46

[87] J.R. Levick. *An introduction to cardiovascular physiology*. Hodder Arnold, London, 2003. 46

[88] Z.R. Struzik, J. Hayano, S. Sakata, S. Kwak, and Y. Yamamoto. **1/f scaling in heart rate requires antagonistic autonomic control**. *Physical Review E*, **70**:050901, 2004. 46

[89] P.C. Ivanov, Z. Chen, K. Hu, and H.E. Stanley. **Multiscale aspects of cardiac control**. *Physica A*, **344**(3-4):685–704, 2004. 47

[90] P. Bak. **Self-organized criticality**. *Physica A*, **163**(1):403–409, 1990. 47

[91] P. Bak. *How nature works: The science of self-organized criticality*. Copernicus, New York, 1996. 47, 50

[92] W.B. Cannon. **Organization for physiological homeostasis**. *Physiological Reviews*, **9**(3):399–431, 1929. 47, 49

[93] A.L. Goldberger. **Is the normal heartbeat chaotic or homeostatic?** *Physiology*, **6**(2):87–91, 1991. 47

[94] J.M. Beggs and D. Plenz. **Neuronal avalanches are diverse and precise activity patterns that are stable for many hours in cortical slice cultures**. *Journal of Neuroscience*, **24**(22):5216–5229, 2004. 47, 50

[95] N. Bertschinger and T. Natschlager. **Real-time computation at the edge of chaos in recurrent neural networks**. *Neural Computation*, **16**(7):1413–1436, 2004. 47, 48, 50

[96] C. Haldeman and J.M. Beggs. **Critical branching captures activity in living neural networks and maximizes the number of metastable states**. *Physical Review Letters*, **94**:058101, 1998. 47, 48, 50

[97] P.E. Latham and S. Nirenberg. **Computing and stability in cortical networks**. *Neural Computation*, **16**(7):1385–1412, 2004. 47

[98] B.H. Friedman and J.F. Thayer. **Anxiety and autonomic flexibility: A cardiovascular approach**. *Biological Psychology*, **47**(3):243–263, 1998. 48

[99] B.H. Friedman. **An autonomic flexibility–neurovisceral integration model of anxiety and cardiac vagal tone**. *Biological Psychology*, **74**(2):185–199, 2007. 48

[100] J.F. Thayer and R.D. Lane. **The role of vagal function in the risk for cardiovascular disease and mortality**. *Biological psychology*, **74**(2):224–242, 2007. 49, 73

[101] D.L. Eckberg. **Parasympathetic cardiovascular control in human disease: a critical review of methods and results**. *American Journal of Physiology- Heart and Circulatory Physiology*, **239**(5):581–593, 1980. 49

[102] H.E. Stanley, L.A.N. Amaral, A.L. Goldberger, S. Havlin, P.C. Ivanov, and C.K. Peng. **Statistical physics and physiology: Monofractal and multifractal approaches**. *Physica A*, **270**(1-2):309–324, 1999. 49

[103] A. Bashan, R. Bartsch, J.W. Kantelhardt, and S. Havlin. **Comparison of detrending methods for fluctuation analysis**. *Physica A*, **387**(21):5080–5090, 2008. 50

[104] D. Delignieres, S. Ramdani, L. Lemoine, K. Torre, M. Fortes, and G. Ninot. **Fractal analyses for 'short' time series: a re-assessment of classical methods**. *Journal of Mathematical Psychology*, **50**(6):525–544, 2006. 50

[105] J.S. Perkiomaki, W. Zareba, F. Badilini, and A.J. Moss. **Influence of Atropine on Fractal and Complexity Measures of Heart Rate Variability**. *Annals of Noninvasive Electrocardiology*, **7**(4):326–331, 2002. 51, 58

[106] M.P. Tulppo, T.H. Makikallio, T. Seppanen, K. Shoemaker, E. Tutungi, R.L. Hughson, and H.V. Huikuri. **Effects of pharmacological adrenergic and vagal modulation on fractal heart rate dynamics**. *Clinical Physiology*, **21**(5):515–523, 2001. 51, 58

[107] S. Akselrod, D. Gordon, J.B. Madwed, N.C. Snidman, D.C. Shannon, and R.J. Cohen. **Hemodynamic regulation: investigation by spectral analysis**. *American Journal of Physiology- Heart and Circulatory Physiology*, **249**(4):867–875, 1985. 52

[108] R.B. Stephenson, O.A. Smith, and A.M. Scher. **Baroreceptor regulation of heart rate in baboons during different behavioral states**. *American Journal of Physiology- Regulatory, Integrative and Comparative Physiology*, **241**(5):277–285, 1981. 52

[109] B. Pomeranz, R.J. Macaulay, M.A. Caudill, I. Kutz, D. Adam, D. Gordon, K.M. Kilborn, A.C. Barger, D.C. Shannon, R.J. Cohen, et al. **Assessment of autonomic function in humans by heart rate spectral analysis**. *American Journal of Physiology- Heart and Circulatory Physiology*, **248**(1):151–153, 1985. 52

[110] E.A. Byrne and S.W. Porges. **Data-dependent filter characteristics of peak-valley respiratory sinus arrhythmia estimation: A cautionary note**. *Psychophysiology*, **30**(4):397–404, 1993. 52

[111] P. Perakakis, M. Taylor, E. Martinez-Nieto, I. Revithi, and J. Vila. **Breathing frequency bias in fractal analysis of heart rate variability**. *Biological Psychology*, **82**:82–88, 2009. 56, 58, 74

[112] L.A. Nunes Amaral, P.C. Ivanov, N. Aoyagi, I. Hidaka, S. Tomono, A.L. Goldberger, H.E. Stanley, and Y. Yamamoto. **Behavioral-independent features of complex heartbeat dynamics**. *Physical Review Letters*, **86**(26):6026–6029, 2001. 58

[113] L.Y.U. Lin, J.L.E.E. Lin, C.C. Du, L.P. Lai, Y.Z.U. Tseng, and S.K.S. Huang. **Reversal of Deteriorated Fractal Behavior of Heart Rate Variability by Beta-Blocker Therapy in Patients with Advanced Congestive Heart Failure**. *Journal of Cardiovascular Electrophysiology*, **12**(1):26–32, 2001. 58

[114] M. Ridha, T.H. Makikallio, G. Lopera, J. Pastor, E. Marchena, S. Chakko, H.V. Huikuri, A. Castellanos, and R.J. Myerburg. **Effects of Carvedilol on Heart Rate Dynamics in Patients with Congestive Heart Failure**. *Annals of Noninvasive Electrocardiology*, **7**(2):133–138, 2002. 58

[115] K.M. Chiu, H.L. Chan, S.H. Chu, and T.Y. Lin. **Carvedilol can restore the multifractal properties of heart beat dynamics in patients with advanced congestive heart failure**. *Autonomic Neuroscience: Basic and Clinical*, **132**(1-2):76–80, 2007. 58

[116] D.T. Schmitt and P.C. Ivanov. **Fractal scale-invariant and nonlinear properties of cardiac dynamics remain stable with advanced age: a new mechanistic picture of cardiac control in healthy elderly**. *AJP-Regulatory, Integrative and Comparative Physiology*, **293**(5):R1923, 2007. 58

[117] C.O. Tan, M.A. Cohen, D.L. Eckberg, and J.A. Taylor. **Fractal properties of human heart period variability: physiological and methodological implications.** *The Journal of physiology*, **15**:3929–3941, 2009. 59

Annex I

Resumen en Español

Introducción

La variabilidad en el ritmo cardiaco (HRV) esta siendo extensivamente estudiada como índice indirecto de la regulación autonómica. En experimentos de psicofisiología, medidas de HRV en estados de reposo se utilizan para elucidar la relación entre estados autonómicos y respuestas emocionales o ejecución de tareas cognitivas. Especialmente las fluctuaciónes del ritmo cardiaco en frecuencias rápidas en sincronía con la respiración sirven como índice del tono vagal, cuya importancia para la salud cardiovascular se ha resaltado en numerosos estudios (para un revisión reciente vease (100)).

La variabilidad cardiaca ha causado recientemente interés entre los expertos del campo de la física estadística que descubrieron que se trataba de una señal compleja y no-lineal. Este descubrimiento provocó una serie de estudios que demostraron que las fluctuaciónes de la tasa cardiaca no son aleatorias sino que se caracterizan por correlaciones que se expanden a largo plazo y no presentan una escala dominante. Esta propiedad de invariabilidad de escala se consideró indicativa de una alta flexibilidad del sistema cardiovascular (2; 55; 66) y condujo al desarrollo de una serie de algorítmos para cuantificar dicha propiedad. De estos algoritmos, el más conocido e utilizado es el "Detrended Fluctuation Analysis" (DFA) que ha sido introducido por Peng y sus colaboradores en 1995, y que desde entonces se ha utilizado en más de 700 estudios de variabilidad cardiaca (26).

Uno de los hallazgos más importantes del estudio de HRV con el método de DFA era la distincíon de la señal cardiaca en dos escalas temporales que presentan propiedades

bien distintas. La primera es la escala de frecuencias rápidas donde las fluctuaciones de la tasa cardiaca están dominadas por las oscilaciones respiratorias, un fenómeno denominado sinus arrítmia respiratorio (RSA) (72). En estas escalas cortas, la aplicación del DFA resulta en exponentes altos, indicativos de altas correlaciones. En frecuencias más lentas, sin embargo, las fluctuaciones de la tasa cardiaca demuestran invariabilidad de escala (26). Aunque la relación entre RSA y las correlaciones en la señal cardiaca se indicó desde el primer articulo de Peng, no existe hasta el presente ningún estudio que explore el efecto preciso de la respiración sobre el "scaling" de la variabilidad cardiaca.

Primer estudio

El primer experimento de la presente tesis investiga el efecto de varios patrones respiratorios sobre los resultados del DFA aplicado a frecuencias rápidas. En el estudio participaron 14 estudiantes universitarios que fueron instruidos en la práctica de tres tipos de frecuencias respiratorias (0.1Hz, 0.2Hz and 0.25Hz), que debían adoptar en el momento indicado. Basados en estudios con señales artificiales que demostraron el efecto de ondas sinusoidales sobre el DFA de señales correlacionadas (68; 69), habíamos trabajado previamente con la hipótesis de que el cambio de frecuencia respiratoria produciría un cambio de "scaling" en una frecuencia correspondiente a la respiratoria.

Los resultados confirmaron la hipótesis y demostraron que la aplicación del DFA en frecuencias rápidas de la señal cardiaca esta sesgada por el RSA. Generalmente, un ritmo respiratorio lento tiende a incrementar los valores del exponente de escalamiento, mientras que frecuencias respiratorias rápidas tienden a reducirlo (111). Como consecuencia, las correlaciones complejas encontradas en las altas frecuencias de las fluctuaciones cardiacas son un mero epifenómeno de los cambios de frecuencia asociados a la respiración, y deben ser distinguidas de las correlaciones intrínsecas de la señal cardiaca, ya que no se corresponden con ellas. Sin embargo, la frecuencia respiratoria tan sólo afecta a las correlaciones complejas a corto plazo en escalas menores al ciclo respiratorio que ha provocado el cambio en el escalamiento. Los registros de la tasa cardiaca en escalas mayores a la frecuencia respiratoria (obtenidos mediante registros de 8 horas o más), pueden contener información fiable acerca de la organización compleja del funcionamiento cardiaco.

Segundo estudio

El segundo estudio presentado en esta tesis examinó el efecto del bloqueo parasimpático sobre los exponentes de escalamiento obtenidos por el DFA. Previamente, varios estu-

dios habían demostrado que la eliminación de la influencia vagal sobre la dinámica cardiaca resulta en un aumento del índice de correlaciones a largo plazo. Sin embargo, ningún estudio previo ofreció una explicación fisiológica para este efecto. Para elucidar la relación entre el tono vagal y los índices del DFA realizamos un experimento donde participaron 9 adultos varones. De estos 9 participantes, 6 recibieron atropina y tres (grupo control) una solución salina como condición placebo. El electrocardiograma continuo se registró durante 10 minutos y los últimos 5 minutos se utilizaron para hallar los índices de variabilidad cardiaca.

Los resultados replicaron las investigaciónes previas que habían encontrado un aumento en el índice de correlaciones después de un bloqueo parasimpático. Sin embargo, en nuestro estudio ofrecimos una nueva interpretación basada en el conocimiento de los efectos de tendencias lineales y sinusoidales sobre el DFA. Nuestra interpretación muestra que el aumento de correlaciones después de bloqueo parasimpático no se debe a alteraciónes en las propiedades intrínsecas de la dinámica cardiaca sino que se trata de un artefacto producido por tendencias locales en la señal.

Programa de análisis

En esta tesis se presenta también un programa informatico de análisis de variabilidad cardiaca denominado "KARDIA" que se desarrolló especificaménte para las necesidades de los estudios previamente descritos. KARDIA se escribió en lenguaje Matlab y esta disponible en codigo abierto a través del repositorio de software libre llamado "SourceForge" (74). El programa incluye funciones tanto para el análisis de respuestas cardiacas fásicas como para el análisis de variabilidad cardiaca en reposo.

Las respuestas fásicas se analizan mediante un promedio ponderado o varios tipos de interpolaciónes. El promedio ponderado se obtiene usando el algoritmo denominado "fractional cycle counts" que esta detalladamente descrito en (40). Este algoritmo es equivalente al metodo propuesto por Graham en 1978 que constituye el procedimiento estándar para el análisis de respuestas cardiacas en el campo de psicofisiología (42). KARDIA también incluye una opción para calcular la respuesta cardiaca de defensa, definida y extensivamente investigada por el grupo de Jaime Vila en la Universidad de Granada (43).

El análisis de variabilidad cardiaca se aplica a segmentos concretos de la señal previamente definidos por el usuario. El programa halla índices comunes del dominio de tiempo como el "root mean square of successive differences". Además, aplica un análisis espectral para obtener medidas de variabilidad en el dominio de frecuencia. Finalmente, el programa incluye el algoritmo de DFA que se aplica en un rango de escalas definido

por el usuario.
La gran ventaja del programa que se esta utilizando actualmente en varios laboratorios en Estados Unidos, España y Brasil, es la capacidad de importar e analizar simultáneamente datos procedentes de varios sujetos. La información de eventos esta importada para cada sujeto individualmente y el programa separa las diferentes condiciónes y exporta los grandes promedios para cada condición en ficheros de Excel. Esta funcionalidad reduce significativamente el tiempo de análisis. Además, KARDIA dispone de varias figuras que se están continuamente actualizando con cada función ejecutada por el usuario, proporcionando un contacto directo con los datos en cada paso del análisis.

Conclusión

La conclusión que se alcanza después de los dos estudios presentados en esta tesis es que la aplicación de índices fractales (o de escalamiento) en un rango de escalas donde la señal cardiaca esta dominada por un mecanismo de control concreto (como por ejemplo el RSA), no es valida. Está demostrado matematicamente que las correlaciones fractales en señales biológicas requieren la interacción antagonista entre los sistemas simpático y parasimpático sumando una entrada de naturaleza aleatoria (84). En un rango de escalas limitado, sin embargo, los parametros de escalamiento son sensibles a tendencias asociadas a mecanismos de control específicos, y no se pueden atribuir a una subyacente organización fractal del sistema cardiovascular. Por esta razón concluimos que la aplicación del DFA a frecuencias rápidas de la señal cardiaca está metodológicamente sesgada y es conceptualmente erronea. Sin embargo, la posibilidad de que el sistema cardiovascular presente una organización fractal en frecuencias más lentas sigue abierta y merece ser investigada rigorosamente.

Annex II

KARDIA Source code: main analysis functions

```
% KARDIA ("heart" in Greek) is a graphic user interface (GUI) designed
% for the analysis of cardiac interbeat interval (IBI) data. KARDIA allows
% interactive importing and visualization of both IBI data and event-related
% information. Available functions permit the analysis of phasic heart rate
% changes in response to specific visual or auditory stimuli, using either
% weighted averages or different interpolation methods (constant, linear,
% spline) at any user-defined sampling rate. KARDIA also provides the user
% with functions to calculate all commonly used time-domain statistics of
% heart rate variability and to perform spectral decomposition by using
% either Fast Fourier Transform or auto-regressive model. Scaling properties
% of the IBI series can also be assessed by means of Detrended Fluctuation
% Analysis. Quantitative results can be easily exported in Excel or MATLAB
% format for further statistical analysis.
%
% To start the GUI type "kardia" in the command window. For usage information
% launch the User's Guide from the toolbox
%
% KARDIA is free software: you can redistribute it and/or modify
% it under the terms of the GNU General Public License as published by
% the Free Software Foundation, either version 3 of the License, or
% (at your option) any later version.
%
% KARDIA is distributed in the hope that it will be useful,
```

```
% but WITHOUT ANY WARRANTY; without even the implied warranty of
% MERCHANTABILITY or FITNESS FOR A PARTICULAR PURPOSE. See the
% GNU General Public License for more details.
%
% You should have received a copy of the GNU General Public License
% along with KARDIA. If not, see <http://www.gnu.org/licenses/>.
%
% This software is freely available at:
% www.ugr.es/~peraka/home/kardia.html
%
% Copyright (C) 2007 2008 Pandelis Perakakis,
% University of Granada
% email: peraka@ugr.es
%
% Update v2.3 - 16/09/2008 - New GUI
%
% Update v2.4 - 30/09/2008 - Unit option in ECP
%
% Update v2.5 - 12/10/2008 - Correct HRV variable order for Excel output
%
% Update v2.6 - 30/10/2008 - Fix concatenation problem in mean algorithm of
% ECP
%
% Update v2.7 - 8/2/2009   - Compatibility with Matlab version 7,
% 'Evoked Cardiac Potentials' changed to 'Phasic Cardiac Responses',
% 'Import' changed to 'Load'


function main_figure = kardia(DATA)



if nargin <1
clearFcn
end

load gui_export.mat
```

—- PCR

———— Select Conditions GUI

```
function PCR_conditions_callback(src,eventdata)
% error when no imported event types are found
if  isempty(DATA.Conditions)
errordlg('No conditions found','PCR')
return
end

% Callbacks
function select_conditions_PCR_callback(src,eventdata)
% get condition indexes
ind=get(list_conditions_PCR,'Value');

% error message
if isempty (ind)
errordlg('No conditions selected','Select Conditions')
return
end

% clear previous results
DATA.GUI.PCRconditions=[];
DATA.GUI.PCRconditionsNum=[];

% update DATA structure
DATA.GUI.PCRconditionsNum=length(ind);
DATA.GUI.PCRconditions=DATA.Conditions(ind);

% update information
update_info_PCR(txt_info_PCR,[]);

delete(PCR_Conditions_Figure)
return
end
```

```
function cancel_conditions_PCR_callback(src,eventdata)
delete(PCR_Conditions_Figure)
end
end

function PCR_callback(src,eventdata)
% get variables
epochstart=str2num(get(edit_epochstart_PCR,'String'));
epochend=str2num(get(edit_epochend_PCR,'String'));
algorithm=get(pop_algorithm_PCR,'Value');
unit=get(pop_unit_PCR,'String');
unitvalue=get(pop_unit_PCR,'Value');
unit=unit{unitvalue};
window=str2num(get(edit_timewindow_PCR,'String'));
baseline=get(check_removebsl_PCR,'Value');
subs=DATA.GUI.SubjectsNum;
SelectedConds=DATA.GUI.PCRconditions;

% pass variables to DATA structure
DATA.GUI.PCR_EpochStart=mat2str(epochstart);
DATA.GUI.PCR_EpochEnd=mat2str(epochend);
switch algorithm
case 1
DATA.GUI.PCR_Algorithm='mean';
case 2
DATA.GUI.PCR_Algorithm='CDR';
DATA.GUI.PCR_EpochStart=mat2str(-15);
DATA.GUI.PCR_EpochEnd=mat2str(80);
case 3
DATA.GUI.PCR_Algorithm='constant';
case 4
DATA.GUI.PCR_Algorithm='linear';
case 5
DATA.GUI.PCR_Algorithm='spline';
end
DATA.GUI.PCR_TimeWindow=mat2str(window);
```

```
DATA.GUI.PCR_Unit=unit;

% error messages
if isempty (epochstart) && ...
algorithm~=2
errordlg('Define epoch limits','PCR')
return
end
if isempty (epochend) && ...
algorithm~=2
errordlg('Define epoch limits','PCR')
return
end
if isempty(DATA.GUI.PCRconditions)
errordlg ('Select conditions first','PCR')
return
end

% clear previous results
DATA.PCR=[];
DATA.PCR_GrandAverage=[];

% use the same eventfile (first subject) for all subjects
if DATA.GUI.SubjectsNum>1 && ...
DATA.GUI.Eventfiles<DATA.GUI.SubjectsNum && ...
isempty(DATA.GUI.UseCommonEventfile);
quest = questdlg(['Do you want to use the first event file'...
' for all subjects?'],'PCR');
switch quest
case 'Yes'
if isempty(DATA.Events(1).Conditions)
errordlg('Load event file for first subject',...
'PCR');
return
end
for i=2:DATA.GUI.SubjectsNum
```

```
DATA.Events(i).Conditions=...
DATA.Events(1).Conditions;
DATA.Events(i).Latencies=...
DATA.Events(1).Latencies;
end
DATA.GUI.UseCommonEventfile=1;
DATA.GUI.Eventfiles=1;
case 'No'
return
case 'Cancel'
return
end
end

for i=1:subs % get subject data
% get necessary variables
data=DATA.Events(i);
if subs==1
Rdata=DATA.R_events;
else
Rdata=DATA.R_events{i};
end
lats=data.Latencies;
conds=data.Conditions;
[hp,t]=ecg_hp(Rdata,'instantaneous');
hr=60*hp.^-1;

for j=1:DATA.GUI.PCRconditionsNum % get condition
index=strcmp(SelectedConds(j),conds);
analysis_lats=lats(index);

HR=[];
BSL=[];
for k=1:length(analysis_lats) % get epoch
lat=analysis_lats(k);
switch algorithm
```

```
case 1 % mean
[HR_mean,HRbsl]=PCR(Rdata,...
lat,lat + epochstart,...
lat + epochend,...
window,unit);
case 2 % CDR
[HRbsl,HR_mean,values]=CDR(Rdata,...
lat,15);
case {3, 4, 5}  % constant, linear, spline
% baseline
HRbsl=ecg_stat(t,lat+epochstart,...
lat,'mean',unit);
% time vector
tt=lat:window:lat+epochend;

if strcmp(unit,'bpm') % switch unit
xx=hr;
elseif strcmp(unit,'sec')
xx=hp;
end

% case constant
if algorithm==3
HR_mean=ecg_interp(t,xx,tt,'constant');
% case linear
elseif algorithm==4
HR_mean=ecg_interp(t,xx,...
tt,'linear');
% case spline
elseif algorithm==5
HR_mean=ecg_interp(t,xx,...
tt,'spline');
end
end
HR=[HR; HR_mean];
BSL=[BSL HRbsl];
```

```
if length(analysis_lats)>1 % average only when more than
% one epochs
HR_mean=mean(HR);
else
HR_mean=HR;
end
HRbsl=mean(BSL);
end

% save results structure
DATA.PCR(i).(SelectedConds{j}).BSL=HRbsl;
DATA.PCR(i).(SelectedConds{j}).HR=HR_mean;
DATA.GUI.PCRepochs(i).(SelectedConds{j})=k;
end
end

% create grand average and data matrix structure
datamatrix=[];
for j=1:DATA.GUI.PCRconditionsNum
baseline=[];
hr=[];
for i=1:subs
baseline=[baseline DATA.PCR(1,i).(SelectedConds{j}).BSL];
hr=[hr; DATA.PCR(1,i).(SelectedConds{j}).HR];
end
dmatrix=[baseline; hr']; % data matrix for one condition
datamatrix=[datamatrix dmatrix]; % data matrix for all conditions
if subs>1
hr=mean(hr);
end
baseline=mean(baseline);
DATA.PCR_GrandAverage.(SelectedConds{j}).BSL=baseline;
DATA.PCR_GrandAverage.(SelectedConds{j}).HR=hr;
end
DATA.GUI.PCRdatamatrix=datamatrix;
```

```
% update plot
plot_PCR(axes_PCR,[]);
update_subjectname_PCR(edit_subjectname_PCR,[]);

% update information
update_info_PCR(txt_info_PCR,[]);
end
```

—- HRV

——— Spectral Analysis

```
function spectral_callback(src,eventdata)
% get variables
samplerate=get(pop_samplerate,'Value');
points=get(pop_points,'Value');
detrendmethod=get(pop_detrendmethod,'Value');
Filter=get(pop_Filter,'Value');
algorithm=get(pop_algorithm_spectral,'Value');
ARorder=str2num(get(edit_ARorder,'String'));
scale=get(pop_scale,'Value');
subs=DATA.GUI.SubjectsNum;
SelectedConds=DATA.GUI.HRVconditions;

switch samplerate
case 1
fs=2;
DATA.GUI.Spectral_SampleRate='2';
case 2
fs=4;
DATA.GUI.Spectral_SampleRate='4';
end

switch scale
case 1
DATA.GUI.Spectral_Scale='normal';
```

```
case 2
DATA.GUI.Spectral_Scale='log';
case 3
DATA.GUI.Spectral_Scale='semilog';
end

ARorder=round(ARorder);
if ARorder>30
errordlg('Choose a smaller model order','Spectral Analysis')
return
end
DATA.GUI.Spectral_ARorder=ARorder';

% error messages
if isempty (DATA.Epochs)
errordlg('Define epochs first','Spectral Analysis')
return
end

% clear previous results
DATA.HRV.Spectral=[];

for i=1:subs % get subject data
% get necessary variables
data=DATA.Epochs(i);

for j=1:DATA.GUI.HRVconditionsNum % get condition
hp=data.(SelectedConds{j}).hp;

% get stats
avIBI=mean(hp*1000);
maxIBI=max(hp*1000);
minIBI=min(hp*1000);
RMS=RMSSD(hp*1000);
SDNN=std(hp*1000);
```

```
hp=hp*1000;
thp=data.(SelectedConds{j}).thp;

% spline interpolation
auxtime = thp(1):1/fs:thp(end);
hp2=(spline(thp,hp,auxtime))';

% detrend hp
switch detrendmethod
case 1
hp3=detrend(hp2,'constant');
DATA.GUI.Spectral_DetrendMethod='constant';
case 2
hp3=detrend(hp2,'linear');
DATA.GUI.Spectral_DetrendMethod='linear';
end

% Filter method
switch Filter
case 1
wdw=hanning(length(hp3));
DATA.GUI.Spectral_Filter='hanning';
case 2
wdw=hamming(length(hp3));
DATA.GUI.Spectral_Filter='hamming';
case 3
wdw=blackman(length(hp3));
DATA.GUI.Spectral_Filter='blackman';
case 4
wdw=bartlett(length(hp3));
DATA.GUI.Spectral_Filter='bartlett';
end

hp4=hp3.*wdw;

% Calculate FFT points
```

```
switch points
case 1
N=512;
DATA.GUI.Spectral_Points='512';
case 2
N=1024;
DATA.GUI.Spectral_Points='1024';
case 3
N=2^nextpow2(length(hp));
DATA.GUI.Spectral_Points=[int2str(N) ' (auto)'];
end

switch algorithm
case 1 % FFT
cw = (1/N) * sum(wdw.^2);
PSD=(abs(fft(hp4,N)).^2)/(N*fs*cw);
F=(0:fs/N:fs-fs/N)';
PSD=2*PSD(1:ceil(length(PSD)/2));
F=F(1:ceil(length(F)/2));
DATA.GUI.Spectral_Algorithm='FFT';

case 2 % AR model
[A, variance] = arburg(hp4,ARorder);
[H,F] = freqz(sqrt(variance),A,N/2,fs);
cw = (1/length(hp4)) * sum(wdw.^2);
PSD= 2*(abs(H).^2)/(fs*cw);
DATA.GUI.Spectral_Algorithm='AR model';
end

% get power in different bands
hf=spPCRower(F,PSD,'hf');
lf=spPCRower(F,PSD,'lf');
vlf=spPCRower(F,PSD,'vlf');
nhf=spPCRower(F,PSD,'nhf');
nlf=spPCRower(F,PSD,'nlf');
```

```
% save results structure
DATA.HRV.Spectral(i).(SelectedConds{j}).PSD=PSD;
DATA.HRV.Spectral(i).(SelectedConds{j}).F=F;
DATA.HRV.Spectral(i).(SelectedConds{j}).HF=hf;
DATA.HRV.Spectral(i).(SelectedConds{j}).LF=lf;
DATA.HRV.Spectral(i).(SelectedConds{j}).VLF=vlf;
DATA.HRV.Spectral(i).(SelectedConds{j}).NHF=nhf;
DATA.HRV.Spectral(i).(SelectedConds{j}).NLF=nlf;
DATA.HRV.Spectral(i).(SelectedConds{j}).avIBI=avIBI;
DATA.HRV.Spectral(i).(SelectedConds{j}).maxIBI=maxIBI;
DATA.HRV.Spectral(i).(SelectedConds{j}).minIBI=minIBI;
DATA.HRV.Spectral(i).(SelectedConds{j}).RMSSD=RMS;
DATA.HRV.Spectral(i).(SelectedConds{j}).SDNN=SDNN;
end
end

% update GUI structure
DATA.GUI.HRV2plot='Spectral';

% update plot
plot_HRV(axes_HRV,[]);
update_subjectname_HRV(edit_subjectname_HRV,[]);
update_condname_HRV(edit_condname_HRV,[]);

% update information
update_info1_HRV(txt_info1_HRV,[]);
end
```

——— DFA

```
function DFA_callback(src,eventdata)
% get variables
minbox=str2num(get(edit_minbox,'String'));
maxbox=str2num(get(edit_maxbox,'String'));
sliding=get(check_slidingwins,'Value');
subs=DATA.GUI.SubjectsNum;
SelectedConds=DATA.GUI.HRVconditions;
```

```
% error messages
if isempty (DATA.Epochs)
errordlg('Define epochs first','DFA')
return
end

% box size restrictions
if ~isint(minbox) || ~isint(maxbox)
errordlg('Box sizes must be integers','DFA')
return
end

if minbox<4
errordlg('Minimum box size is 4','DFA')
return
end

% clear previous results
DATA.HRV.DFA=[];

for i=1:subs % get subject data
% get necessary variables
data=DATA.Epochs(i);

for j=1:DATA.GUI.HRVconditionsNum % get condition
hp=data.(SelectedConds{j}).hp;

% get stats
avIBI=mean(hp*1000);
maxIBI=max(hp*1000);
minIBI=min(hp*1000);
RMS=RMSSD(hp*1000);
SDNN=std(hp*1000);

switch sliding
```

```
case 1 % Use Sliding Windows
[a,n,Fn]=DFA(hp,minbox,maxbox,'s',0);
DATA.GUI.DFA_sliding='Yes';
case 0 % Non sliding windows
[a,n,Fn]=DFA(hp,minbox,maxbox,0,0);
DATA.GUI.DFA_sliding='No';
end

% save results structure
DATA.HRV.DFA(i).(SelectedConds{j}).a=a;
DATA.HRV.DFA(i).(SelectedConds{j}).n=n;
DATA.HRV.DFA(i).(SelectedConds{j}).Fn=Fn;
DATA.HRV.DFA(i).(SelectedConds{j}).avIBI=avIBI;
DATA.HRV.DFA(i).(SelectedConds{j}).maxIBI=maxIBI;
DATA.HRV.DFA(i).(SelectedConds{j}).minIBI=minIBI;
DATA.HRV.DFA(i).(SelectedConds{j}).RMSSD=RMS;
DATA.HRV.DFA(i).(SelectedConds{j}).SDNN=SDNN;
end
end

% update GUI structure
DATA.GUI.HRV2plot='DFA';
DATA.GUI.DFA_minbox=mat2str(minbox);
DATA.GUI.DFA_maxbox=mat2str(maxbox);

% update plot
plot_HRV(axes_HRV,[]);
update_subjectname_HRV(edit_subjectname_HRV,[]);
update_condname_HRV(edit_condname_HRV,[]);

% update information
update_info1_HRV(txt_info1_HRV,[]);
end
```

———- AUXILARY FUNCTIONS ———

—- CDR

```
function [baselineHR,medians,Vsec]=CDR(sig,TS,baseline)
% transpose data vector
if size(sig,1)>size(sig,2)
sig=sig';
end

% create heart period vector
[hp,t]=ecg_hp(sig,'instantaneous');

% define T0 to calculate baseline heart rate
T0=TS-baseline;
baselineHR=ecg_stat(t,T0,TS,'mean','bpm'); % baseline Heart Rate

% calculate mean heart rate sec by sec
Vsec=[];
count=0;
for i=1:80
V=ecg_stat(t,TS+count,TS+i,'mean','bpm');
count=count+1;
Vsec=[Vsec V];
end

% calculate medians
medians=[median(Vsec(1:3)) median(Vsec(4:6)) median(Vsec(7:11)) ...
median(Vsec(12:16)) median(Vsec(17:23)) median(Vsec(24:30))...
median(Vsec(31:37)) median(Vsec(38:50)) median(Vsec(51:63))...
 median(Vsec(64:76))];
end
```

—- PCR

```
function [HRmean,HRbsl]=PCR(t,TS,T0,T1,step,unit)

% get heart period
```

```
[hp,t]=ecg_hp(t,'instantaneous');

% calculate baseline HR
HRbsl=ecg_stat(t,T0,TS,'mean',unit); % call ecg_stat

% calculate mean HR changes in variable window sizes defined
% by step
window=round(T1-TS); % analysis window length
nboxes=floor(window/step); % number of boxes that fit in
% analysis window
HRmean=[];
count=0;
for i=1:nboxes
mhr=ecg_stat(t,TS+count*step,TS+step*i,'mean',unit);
count=count+1;
HRmean=[HRmean mhr];
end
end
```

—- DFA

```
function [alpha,n,Fn]=DFA(y,varargin)
% set default values for input arguments
sliding=0;
graph=0;
minbox=4;
maxbox=floor(length(y)/4);

% check input arguments
nbIn = nargin;
if nbIn > 1
if ~ischar(varargin{1})
minbox = varargin{1};
if ~ischar(varargin{2})
maxbox = varargin{2};
else
error('Input argument missing.');
```

```
end
end
for i=1:nbIn-1
if isequal (varargin{i},'plot'), graph='plot';end
if isequal (varargin{i},'s'), sliding='s';end
end
end

if nbIn > 5
error('Too many input arguments.');
end

% initialize output variables
alpha=[];
n=NaN(1,maxbox-minbox+1);
Fn=NaN(1,maxbox-minbox+1);

% transpose data vector if necessary
s=size(y);
if s(1)>1
y=y';
end

% substract mean
y=y-mean(y);

% integrate time series
y=cumsum(y);

N=length(y); % length of data vector

% error message when box size exceeds permited limits
if minbox<4 || maxbox>N/4
disp(...
[mfilename ': either minbox too small or maxbox too large!']);
return
```

```
end

% begin loop to change box size
count=1;
for n=minbox:maxbox;
i=1;
r=N;
m=[];
l=[];

% begin loop to create a new detrended time series using boxes
% of size n starting from the beginning of the original time
% series
while i+n-1<=N % create box size n
x=y(i:i+n-1);
x=detrend(x); % linear detrending
m=[m x];
if strcmp(sliding,'s')
i=i+1; % sliding window
else
i=i+n; % non-overlapping windows
end
end

% begin loop to create a new detrended time series with
% boxes of size
% n starting from the end of the original time series
while r-n+1>=1
z=y(r:-1:r-n+1);
z=detrend(z);
l=[l z];
if strcmp(sliding,'s')
r=r-1;
else
r=r-n;
end
```

```
end

% calculate the root-mean-square fluctuation of the new
% time series
k=[m l]; % concatenate the two detrended time series
k=k.^2;
k=mean(k);
k=sqrt(k);
Fn(count)=k;
count=count+1;
end

n=minbox:maxbox;

% plot the DFA
if strcmp (graph,'plot');
figure;
plot(log10(n),log10(Fn))
xlabel('log(n)')
ylabel('log(Fn)')
title('Detrended Fluctuation Analysis')
end

% calculate scaling factor alpha
coeffs= polyfit(log10(n),log10(Fn),1);
alpha = coeffs(1);

end
```

—- RMSSD

```
function y=RMSSD(sig)

dsig=diff(sig);
y=dsig.^2;
y=sqrt(mean(y));
end
```

—- spPCRower

```
function power=spPCRower(F,PSD,freq)
% define frequency bands
vlf=0.04; % very low frequency band
lf=0.15; % low frequency band
hf=0.4; % high frequency band

% calculate number of points in the spectrum
N=length(PSD);
%calculate maximum frequency
maxF=F(2)*N;

if hf>F(end),
hf=F(end);
if lf>hf,
lf=F(end-1);
if vlf>lf,
vlf=F(end-2);
end
end
end

%calculate limiting points in each band
index_vlf=round(vlf*N/maxF)+1;
index_lf=round(lf*N/maxF)+1;
index_hf=round(hf*N/maxF)+1;
if index_hf>N,index_hf=N;end

switch freq
case {'total'}
% calculate total energy (from 0 to hf) in ms^2
total=F(2)*sum(PSD(1:index_hf-1));
power=total;
case {'vlf'}
%calculate energy of very low frequencies (from 0 to vlf2)
vlf=F(2)*sum(PSD(1:index_vlf-1));
```

```
power=vlf;
case {'lf'}
%calculate energy of low frequencies (from vlf2 to lf2)
lf=F(2)*sum(PSD(index_vlf:index_lf-1));
power=lf;
case {'hf'}
%calculate energy of high frequencies (from lf2 to hf2)
hf=F(2)*sum(PSD(index_lf:index_hf-1));
power=hf;
case {'nlf'}
%calculate normalized low frequency
lf=F(2)*sum(PSD(index_vlf:index_lf-1));
hf=F(2)*sum(PSD(index_lf:index_hf-1));
nlf=lf/(lf+hf);
power=nlf;
case {'nhf'}
%calculate normalized low frequency
lf=F(2)*sum(PSD(index_vlf:index_lf-1));
hf=F(2)*sum(PSD(index_lf:index_hf-1));
nhf=hf/(lf+hf);
power=nhf;
otherwise
disp('Uknown frequency range selection')
power=nan;
end
end
```

Declaration

I herewith declare that I have produced this paper without the prohibited assistance of third parties and without making use of aids other than those specified; notions taken over directly or indirectly from other sources have been identified as such. This paper has not previously been presented in identical or similar form to any other Spanish or foreign examination board.

The thesis work was conducted from 2006 to 2009 under the supervision of Jaime Vila Castellar, Gustavo Reyes del Paso and Lourdes Anllo-Vento at the University of Granada.

Granada, 1 of October 2009